Spectral Analysis of Non-linear, Non-stationary Time Series Data Using Hilbert-Huang Transform and Spectrogram

Studienarbeit Report

Submitted for the degree of
Master of Science in Mechatronics
by

Vishu Sharma
Matriculation Nr: 1523731

The Chair of Mechanics
Structural Health Monitoring
Faculty IV

March 2024

Supervisor: Prof. Dr.-Ing. Peter Kraemer

Abstract

This research project aims to explore and compare the effectiveness of Fourier Spectral Analysis (FSA), including Fourier Transform and Spectrogram, alongside Hilbert Huang Transform (HHT) and Hilbert Spectral Analysis (HSA) in analyzing non-linear and non-stationary time series signals. This research investigates the intricacies of FSA, HHT, and HSA with an in-depth discussion of their mathematical background, working, and limitations with examples.

The research applies these methods/frameworks to analyze both synthetic and natural signals and extracts valuable insights by comparing the performance of the two frameworks. This research also explores the limitations of traditional Fourier Spectral Analysis when dealing with non-stationary and non-linear signals and demonstrates the effectiveness of HHT in providing better time-frequency resolution.

The research includes practical applications to real-world sensor data from off-shore wind turbines such as accelerometers, showcasing the potential application of these methods in various scientific and engineering disciplines. This research also scrutinizes the limitations of HHT and examines recent advancements in the field aimed at addressing these challenges.

Key Words: Time Series, Fourier Spectral Analysis, Hilbert Huang Transform, Spectrogram, Empirical Mode Decomposition, Intrinsic Mode Functions.

Declaration of Independent Work

I, Vishu Sharma, hereby declare that the work done in this Studienarbeit titled "Spectral Analysis of Non-linear, Non-stationary Time Series Data Using Hilbert-Huang Transform and Spectrogram " is my own work and it has not been previously submitted for any degree or other purposes. Furthermore, all sources that assisted me throughout this project, including other researchers' work published, have been fully cited.

....

Siegen, 18.03.2024

Contents

List of Figures

CHAPTER 1

Introduction

1.1 Time Series

A time series is defined as an ordered sequence of values of a variable at equally spaced time intervals. Some examples of time series are the price of commodities over time, human speech, and temperature change over time. Figure 1.1 shows the variation of mean annual temperature in Germany from the 1900s to 2020. This data is obtained from World Bank Climate Knowledge Portal. Time series analysis is important for obtaining underlying patterns in natural processes and dynamical systems. These patterns obtained by time series data analysis can be used to make predictions in many disciplines of science and engineering. One example of such discipline is vibration-based condition monitoring of rotating machines. By analyzing the time-series data obtained from accelerometers installed on rotating machines, predictions can be made regarding damage detection and the machine's health.

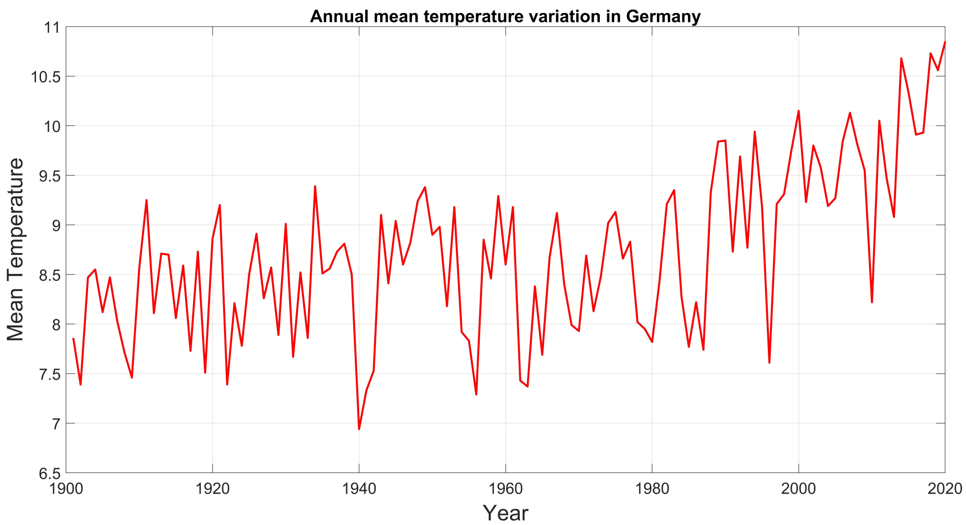

Figure 1.1: Annual mean temperature variation in Germany from 1901 to 2021 as time series

Methods to analyze time series can be broadly categorized into two classes; Time domain and Frequency domain. Examples of some time domain methods are correlation analysis, Auto Regression (AR), Moving Average (MA), and ARMA models, etc. Frequency domain methods include Fourier spectral analysis, Hilbert spectral analysis, and wavelet analysis. Time-frequency domain methods are a combination of both Time and Frequency domain methods. The spectrogram is an example of one such method. This report is focused on Fourier spectral analysis and Hilbert-Huang Transform. It is assumed that the reader is already familiar with the Fast Fourier Transform and its application in signal processing. Nonetheless, chapter 2 discusses Fourier spectral analysis in brief with some examples to illustrate its advantages and limitations.

1.2 Stationarity

A time series is called weak stationary if its mean, variance, and auto-correlation function are constant over time t. The Definition of the weak stationarity for a time series X(t) is given by:

$$E(|X(t)^2)|) < \infty \tag{1.1}$$

$$E(X(t)) = m \tag{1.2}$$

$$C(X(t_1), (X(t_2)) = C(X(t_1 + \tau), X(t_2 + \tau)) = C(t_1 - t_2) \tag{1.3}$$

Where E(.) is the expected value of the quantity, C(.) is the auto-correlation function. This stationarity is also referred to as covariance stationarity or second-order stationarity. Another definition of stationarity called piece-wise stationarity is less rigorous. It applies when a random variable is stationary for a limited time span but the scale/time span is not specified.

1.3 Non-Linearity

In this report, non-linearity refers to the non-linearity generated from interaction between modes and within modes. This non-linearity is generated by two different mechanisms: intra-mode and inter-mode interactions depending on the additive and multiplicative interaction between modes. Non-linear processes exhibit frequency modulation(FM) and amplitude modulation(AM). Intra-mode frequency modulation occurs when the instantaneous frequency changes within one oscillation cycle. Inter-mode frequency modulation occurs when two or more different modes present in the signal interact with each other. The multiplicative interaction between modes results in energy spreading throughout the frequency range in the Fourier spectrum. [10] [11].

1.4 Examples of Non-linearity and Non-stationarity

The signals represented by the following equations illustrate the concepts of non-linearity, non-stationarity, additive, and multiplicative interaction between modes.

$$x_1(t) = 2.0 \times \sin(5 \cdot 2\pi t) + 1.0 \times \sin(3 \cdot 2\pi t) + Noise \tag{1.4}$$

$$x_2(t) = 2.0 \times e^{-0.05t} \times \sin(5 \cdot 2\pi t) + 1.0 \times \sin(3 \cdot 2\pi t) + Noise \tag{1.5}$$

$$x_3(t) = 2.0 \times \sin(5 \cdot 2\pi t) \times \sin(3 \cdot 2\pi t) + Noise \tag{1.6}$$

$$x_4(t) = 2.0 \times e^{-0.05t} \times \sin(5 \cdot 2\pi t) \times \sin(3 \cdot 2\pi t) + Noise \tag{1.7}$$

The signal represented by the first equation 1.4 is linear and stationary. In this signal, there is only additive interaction between modes. The signal given by the equation 1.5 is non-stationary but linear. Non-stationarity is due to the exponential decay and it is linear due to additive interaction between modes. The third signal represented by the equation 1.6 is non-linear but stationary. It has a multiplicative interaction between modes and this type of interaction leads to inter-mode non-linearity. Finally, the signal represented by the equation 1.7 is non-stationary as well as non-linear.

1.5 Hilbert Huang Transform

The Hilbert Huang Transform (HHT) was first proposed by Norden E. Huang at Goddard Space Flight Center (GSFC), NASA [12]. It was developed to deal with natural processes which are non-linear and non-stationary in nature. Existing methods like spectrogram, Wigner-Ville, and wavelet analysis are suitable for data that is linear but non-stationary. HHT allows spectrum analysis of non-linear and non-stationary data. Non-linear processes need special treatment. In non-linear processes dynamics of the underlying system are also important other than periodicity. HHT consists of two parts:

1. Empirical Mode Decomposition (EMD),
2. Hilbert Spectral Analysis (HSA).

The key part of the method is the EMD. With EMD, time series data/signal can be decomposed into a small number of intrinsic mode functions (IMFs). The decomposition is based on the local characteristic time scale of the data. This method is local and adaptive. With the Hilbert transform, the IMF yields instantaneous frequencies as functions of time. Performance comparisons with Fourier spectral analysis show that the HHT offers better temporal and frequency resolutions for non-linear and non-stationary data. For strictly linear and stationary data, the Fourier spectral analysis produces superior results.

CHAPTER 2

Signal Processing based on Fourier Spectral Analysis

2.1 Fourier Series

According to Fourier series, any periodic signal $x(t)$, can be decomposed into a linear combination of sines, cosines and its harmonics.

$$x(t) = \frac{A_0}{2} + \sum_{n=1}^{\infty}(A_n cos(n\omega t) + B_n sin(n\omega t)) \tag{2.1}$$

These sinusoids have a fundamental frequency ω with T as period.

$$\omega = \frac{2\pi}{T} \tag{2.2}$$

The Fourier coefficients A_n and B_n are given by:

$$A_n = \frac{2}{T}\int_0^T x(t) cos(\omega nt)\, dt \tag{2.3}$$

$$B_n = \frac{2}{T}\int_0^T x(t) sin(\omega nt)\, dt \tag{2.4}$$

$x(t)$ can also be written in discrete Fourier representation with complex coefficients C_n as:

$$x(t) = \sum_{n=1}^{\infty} C_n e^{i\omega nt} \tag{2.5}$$

$$e^{i\omega nt} = cos(\omega nt) + icos(\omega nt) \tag{2.6}$$

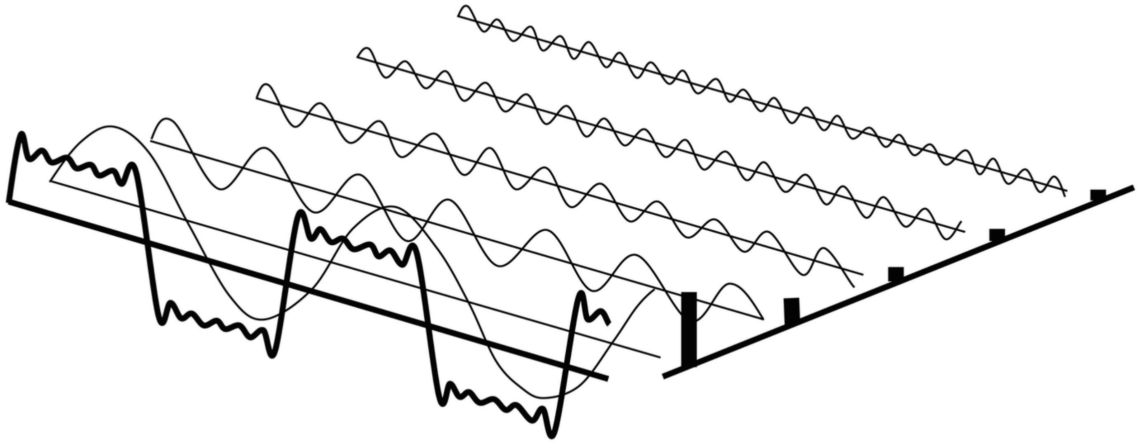

Figure 2.1: Fourier Decomposition of Signal $x(t)$ into sinusoids

Figure 2.1 shows how a time a signal $x(t)$ can be decomposed into a number of sinusoids with Fourier coefficients representing the magnitude of these sinusoids. Source of the figure can be found here [23].

2.2 Fourier Transform

Fourier Transform is closely related to Fourier series. Fourier series was defined for periodic functions. In Fourier transform, the period T extends from $-\infty$ to ∞. After applying Fourier Transform to a signal, it is transformed from time domain to the frequency domain. This frequency domain representation is known as the Fourier spectrum.

$$X(\omega) = \frac{1}{2\pi} \int_{-\infty}^{\infty} x(t) e^{-i\omega t}\, dt \tag{2.7}$$

In equation 2.7, $x(t)$ is signal in time domain, $X(\omega)$ is complex and represents the spectrum in frequency domain. The term exp(.) contains the basis function.

Fourier spectrum of signal defines uniform harmonic components globally with assumed basis as trigonometric functions (sines and cosines). A superposition of these uniform harmonic components is used to represent the data. This superposition is linear and additive.

2.3 Discrete Fourier Transform

Discrete Fourier Transform (DFT) is a discretized version of the Fourier series obtained by discretizing the signal $x(t)$ at equidistant time intervals. A n-point DFT for input signal x transforms it to frequency domain X. It is given by:

$$X_k = \sum_{j=0}^{n-1} x_j e^{-i2\pi jk/n} \tag{2.8}$$

This output vector X_k contains the Fourier coefficients for input vector x. Output vector contains both magnitude and phase. In the matrix notation it can be written as:

$$
\begin{bmatrix} X_1 \\ X_2 \\ X_3 \\ . \\ . \\ X_n \end{bmatrix} = \begin{bmatrix} 1 & 1 & 1 & . & . & 1 \\ 1 & W_n & W_n^2 & . & . & W_n^{n-1} \\ 1 & W_n^2 & W_n^4 & . & . & W_n^{2(n-1)} \\ . & . & . & . & . & . \\ . & . & . & . & . & . \\ 1 & W_n^{n-1} & W_n^{2(n-1)} & . & . & W_n^{2(n-1)^2} \end{bmatrix} \begin{bmatrix} x_1 \\ x_2 \\ x_3 \\ . \\ . \\ x_n \end{bmatrix}
$$

where W_n is the n-th root of unity, since $e^{-i2\pi}$ is equal to 1 from Euler's formula.

$$
W_n = e^{-i2\pi/n} \tag{2.9}
$$

The above stated matrix multiplication for DFT can be written in compact form as equation 2.10. Here F_n is a complex valued matrix of dimension n x n. It is also called the DFT matrix or Fourier matrix.

$$
X = F_n.x \tag{2.10}
$$

Computing DFT involves n x n multiplication operations. DFT is a linear operator. As n increases, the computational complexity scales as O(n^2). For example, to compute DFT for a signal with 10,000 sampling points, (10^8) 100 million multiplication operations needs to be performed! This is computationally expensive and not very efficient.

2.4 Fast Fourier Transform

Fast Fourier Transform (FFT) is the high performance digital equivalent of DFT. FFT allows the efficient computation of Fourier-transform on digital computers. It has been one of the most successful tools in signal processing in the last five decades. It was proposed by James W. Cooley and John W. Tukey in 1965 in the paper titled "An Algorithm for the Machine Calculation of Complex Fourier Series" [7] [4]. Radix-2 DIT (decimation in time) FFT is the most common form of Cooley-Tookey algorithm and is widely used in signal processing. Although the history for calculating FFT can be traced back to Carl Friedrich Gauss as early as in 1805.

Properties of DFT Matrix exploited by FFT

The DFT matrix F_n has some remarkable properties. These properties are exploited by FFT algorithms to reduce the computational complexity while using DFT in signal processing applications [5].

- The most remarkable property is that a higher order DFT matrix F_n of dimension $n \times n$ can be substituted with 2 low dimension DFT matrix of dimension $n/2$ in computations.
- For example, a DFT matrix F_{64} of size 64×64 can be substituted with two smaller DFT matrices of size 32×32 in computation. These smaller F_{32} DFT matrices of size 32×32 can be further substituted by even smaller F_{16} DFT matrices of size 16×16 .
- This reduces the (64^2) multiplication operations required in the original F_{64} DFT matrix to $2 \times (32^2)$ in F_{32} DFT matrix. FFT scales as O($nlog(n)$). To implement

FFT, the number of data points n should be taken as a power of 2. If n is not a power of 2, then n should be padded with zeroes to make it a power of 2 .

2.5 Examples based on Fast Fourier Transform

Consider an artificial/synthetic stationary signal shown in figure 2.2 sampled at 500Hz with 2000 data points and defined by the equation :

$$x(t) = 10\sin(15 \times 2\pi t) + 7\sin(30 \times 2\pi t) + 5\sin(50 \times 2\pi t) + 3\cos(100 \times 2\pi t) + Noise \tag{2.11}$$

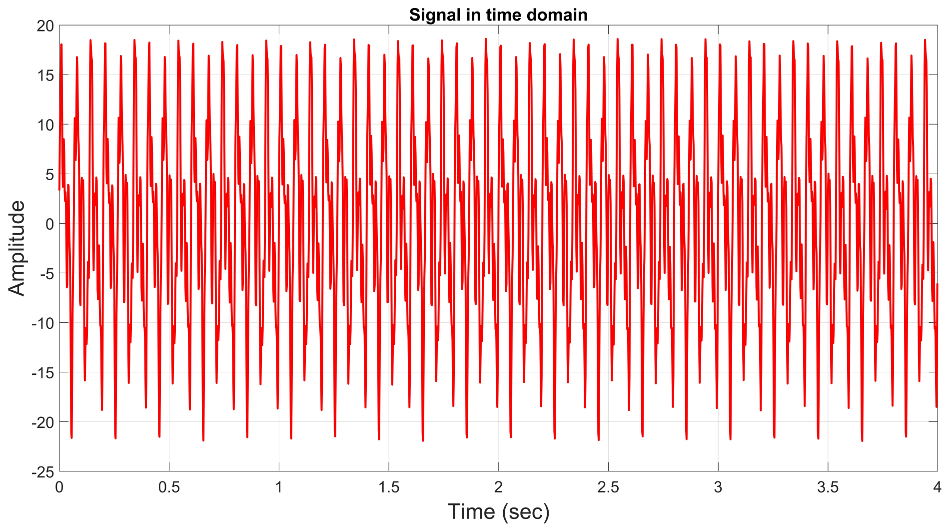

Figure 2.2: Stationary signal in time domain

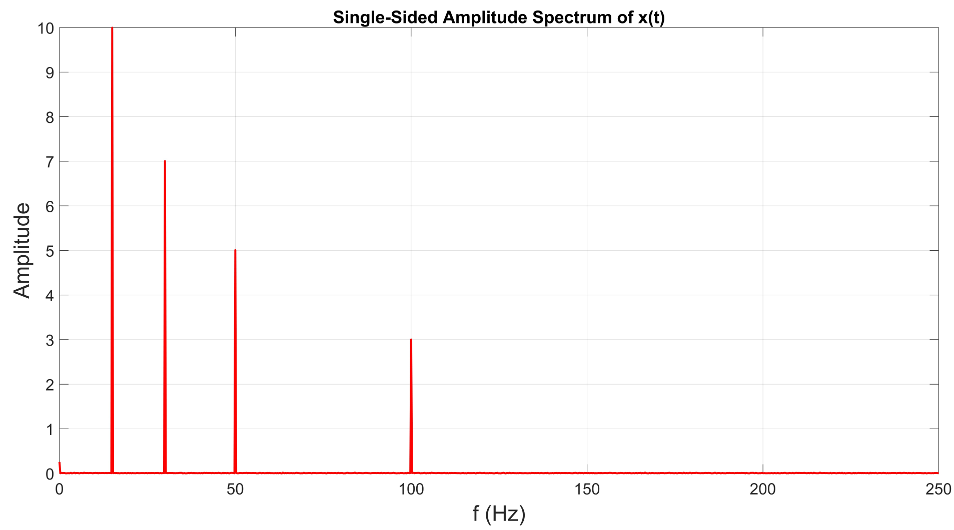

Figure 2.3: Spectrum of a stationary signal in frequency domain

It was difficult to guess the frequency content of this signal in the time domain. But in the frequency domain, a very good resolution in frequency can be obtained using Fourier spectral analysis. Signal components of frequency 15, 30, 50, and 100 Hz with amplitudes 10, 7, 5, and 3 units can be identified with relative ease as shown in figure 2.3.

Consider another example of a signal sampled at 0.4Hz with 128 data points and defined by the equation:

$$x(t) = 100 \cos(2\pi(0.04)t) + 205 \cos(2\pi(0.07)t) \tag{2.12}$$

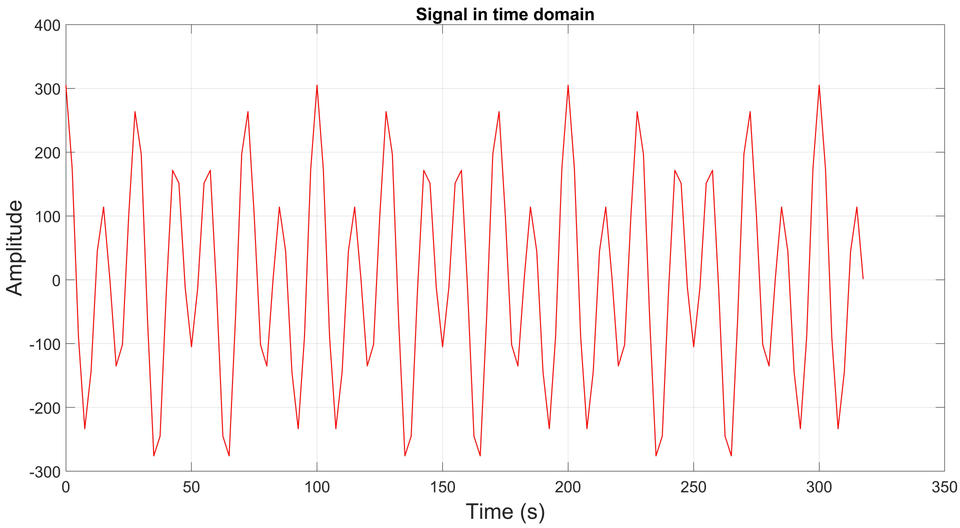

Figure 2.4: Signal in time domain

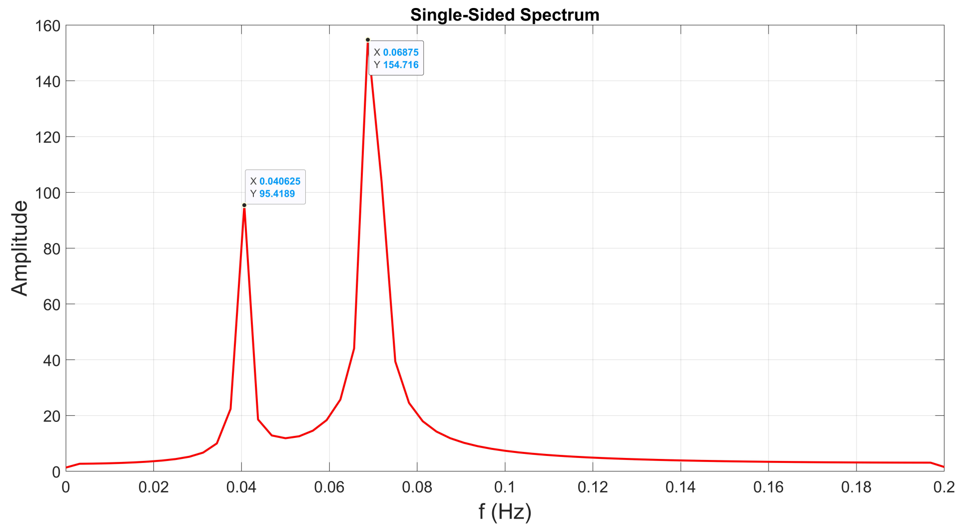

Figure 2.5: Single sided spectrum of signal with leakage

In the Fourier spectrum of this signal, as shown in figure 2.5, it can be noticed that the amplitude is reduced to 95.4 from 100 units for frequency the of 0.04 Hz. Similarly, for the frequency 0.07 Hz, the amplitude has been reduced to 154.7 from 205 units! A significant amount of energy is leaked and smeared across frequencies that do not occur originally in the spectrum.

If the same signal is sampled at 0.4Hz but with 5000 data points. It can be easily noticed from figure 2.6 that, the Fourier spectrum shows no leakage. Here frequency resolution is significantly better and the amplitude of frequency components in the spectrum doesn't get reduced (leaked). To get a better resolution in frequency and to reduce this energy spreading, more data points i.e. a longer signal in time is required!

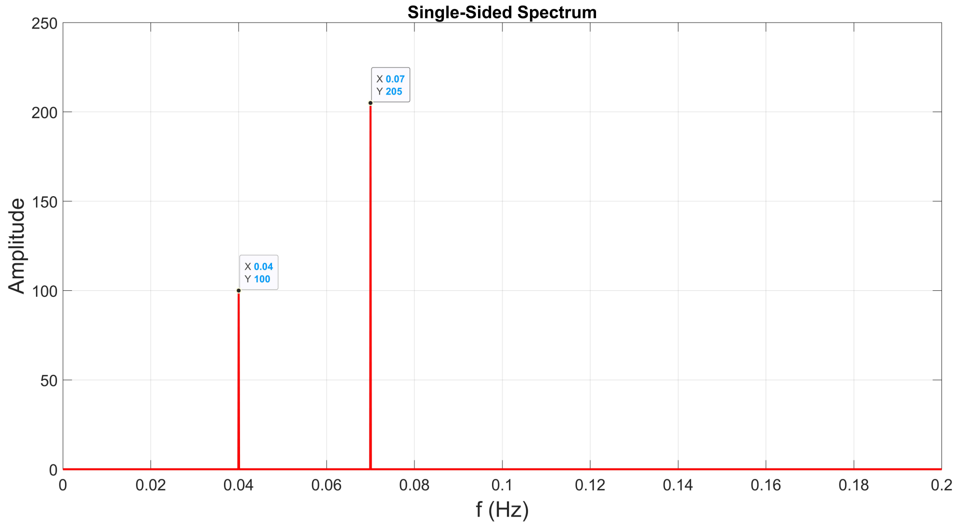

Figure 2.6: Single sided spectrum of signal with reduced leakage

2.6 Short Time Fourier Transform (Spectrogram)

Spectrogram or STFT (Short Time Fourier Transform) is a Fourier spectral analysis with a limited width time window. Spectrograms divide the input signal into time-windows and then compute the Fourier transforms of those time-windows. The spectrogram is one of the most frequently used time-frequency representations of signal. It is given by the equation below with $w(t\text{-}\tau)$ as limited time window:

$$X_{ST}(t,\omega) = \frac{1}{2\pi}\int_{-\infty}^{\infty} x(t)w(t-\tau)e^{-i\omega t}\,dt \tag{2.13}$$

Sometimes the representation of the signal in time or frequency domain alone is not sufficient to describe the physical situation about what is happening in the signal. Spectrograms can help in describing how the spectral content of a signal changes in time. Spectrograms assume the data to be piece-wise stationary and try to achieve some localization in time by using fixed-length windows. The size of the window should be long enough to capture at least one cycle of a component frequency. The window size to be used in the spectrogram should not be too large, otherwise it would lead to a bad temporal resolution. To better understand the application of spectrogram, some examples are used in the following sections.

Spectral Analysis of Sputnik's Audio recording based on STFT

Consider an example of a non-stationary signal as shown in figure 2.7 from the first artificial Earth satellite Sputnik 1's beep, recorded as audio and sampled at 48kHz. Source of the data can be found here Sputnik audio

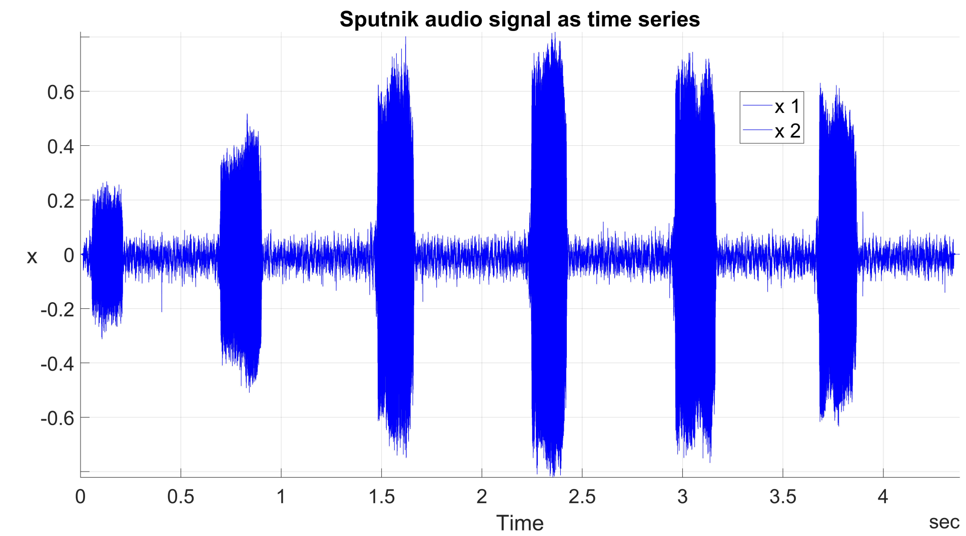

Figure 2.7: Audio signal from Sputnik 1 in time domain

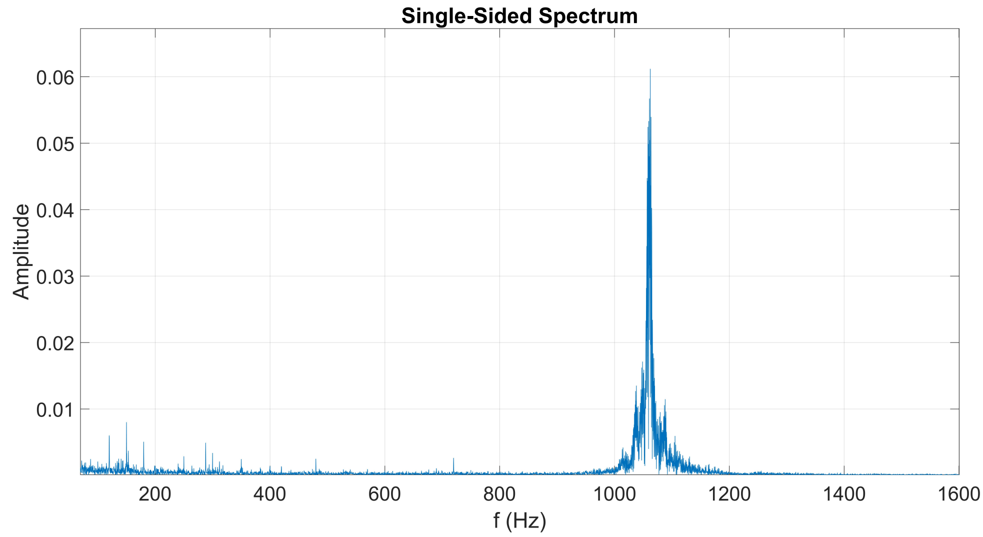

Figure 2.8: Frequency spectrum of Sputnik 1's audio

The audio signal in the time domain as shown in figure 2.7 gives a very good idea about when the beep is taking place but no idea about the frequency components contained in it. On the other hand, if we look at the signal in the frequency domain we can easily identify the dominating frequency components (f = 1056 Hz to 1064 Hz) in the signal. However, there is no information about the time, when these frequency components are occurring in the signal. We do not know if the above-mentioned frequency components occur throughout the signal or occur sporadically. To see both, the frequency components and when they are occurring in time, the spectrogram of the signal is used in further analysis.

This analysis as shown in figure 2.9 is produced using a blackman window with 1024 samples and 50 percent overlap. The minimum threshold (For signal to noise ratio) was kept at -60 dB/Hz for PSD to reject noise below this power level. No scaling factor for

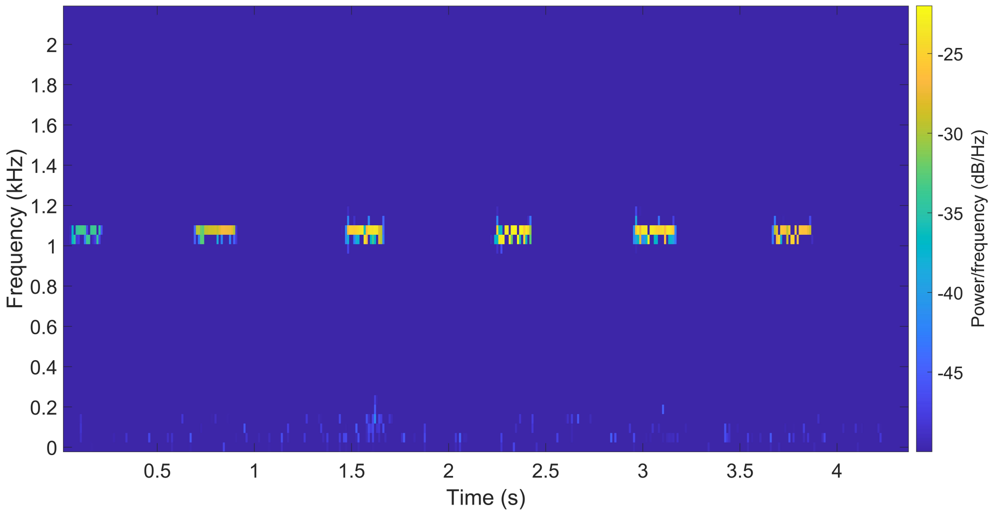

Figure 2.9: Spectrogram of Sputnik 1's audio

energy/amplitude is used since the absolute value of the amplitude is not the focus of the discussion. From this spectrogram, we can see that the dominating frequency components (around 1.06 kHz) occur approximately at 0.12, 0.83, 1.62, 2.33, 3.04, and 3.77 seconds with the highest amplitude at 2.33 seconds. This can be easily verified by looking at the signal in the time domain. The spectrogram gave a good resolution in both the time and frequency domain.

2.7 Limitations of Signal Processing methods based on Fourier Spectral Analysis

Most real-life signals that occur in nature are non-stationary, non-linear, and have multiple frequency components. Despite its success, Fourier spectral analysis has some crucial restrictions:

- System must be linear
- Data must be stationary

If these conditions are not met, the resulting spectrum from the Fourier spectral analysis will be misleading and less meaningful for the signal analysis.

The idea behind the spectrogram is to divide the original signal into smaller segments (windows) and analyze each segment by means of Fourier spectral analysis. This window/kernel moves as if it is sliding over the entire signal. How large the window size is and how much it overlaps can be controlled, but it remains fixed once chosen. Now the question arises what is the optimal window size? Also once the window is selected how to know if the window size is compatible with time-scales in data? Is there a limit to how small we can make these segments? Will the resulting time-frequency distribution be still meaningful if we keep decreasing window size?

The chosen window size does not always coincide with the stationary time scales present in the signal. It is hard to localize an event in time for good frequency resolution with a narrow window. Leon Cohen in his book titled "Time-Frequency Analysis" suggests that after making these segments smaller (narrower window) up to a certain limit the spectrum becomes meaningless. It does not represent the spectrum of the original signal. Cohen recommends, that to get a good frequency resolution, this energy spreading should be minimized around the estimated instantaneous frequency. The ideal window should be such that the local standard deviation is minimum. [6]

Still, one of the drawbacks of STFT remains i.e. the presence of a fixed window. Non-stationarity and non-linearity in the signal can induce spurious harmonic components that cause energy spreading. The consequence is the misleading energy–frequency distribution for non-linear and non-stationary data. These spurious harmonics and the wide frequency spectrum cannot faithfully represent the true energy density in the frequency domain [12]. How the non-linearity (inter-mode) affects the frequency spectrum of the signal is illustrated with examples in Chapter 4.

To understand the drawbacks of the time-frequency analysis by spectrogram in more detail, the concept of degree of stationarity (quantitative) and instantaneous frequency is discussed in the next chapter.

CHAPTER 3

Signal Processing based on Hilbert-Huang Transform

3.1 Instantaneous Frequency

If a frequency changes from time to time within a wave, its profile can no longer be a simple sine or cosine function. Any wave-profile deformation from the simple sinusoidal leads to distortions known as intrawave frequency modulation. It indicates that the instantaneous frequency changes within one oscillation cycle. In Fourier spectral analysis, we need at least one full oscillation of a sine or a cosine wave to define the local frequency value. According to this logic, nothing shorter than a full wave will do. Such a definition would not make sense for non-stationary data for which the frequency has to change values from time to time [12].

The instantaneous frequency characterizes a local frequency behavior as a function of time [1]. A more general definition of Instantaneous frequency is given by Leon Cohen [6]. It is defined as the derivative of the phase of the analytical signal. This definition is based on moments of spectrum.

Consider an analytical signal given by the equation:

$$z(t) = x(t) + iy(t) \tag{3.1}$$

$$z(t) = a(t)e^{i\theta(t)} \tag{3.2}$$

$$a(t) = \sqrt{x^2(t) + y^2(t)} \tag{3.3}$$

$$\theta(t) = \arctan \frac{y(t)}{x(t)} \tag{3.4}$$

Where $y(t)$ is Hilbert Transform of $x(t)$, $a(t)$ is the envelope signal, $\theta(t)$ is instantaneous phase signal. The reason for using a complex signal is that the phase and amplitude of a signal can be obtained unambiguously. An expression for instantaneous frequency can also be derived using a complex signal. Calculating instantaneous frequency from data is difficult because it is the time derivative of $\theta(t)$. If $S(\omega)$ is the spectrum of $z(t)$, then the mean frequency is given by:

$$< \omega >= \int_0^\infty \omega |S(\omega)|^2 \, d\omega \tag{3.5}$$

$$< \omega >= \int z^*(t) \frac{1}{i} \frac{d}{dt} z(t) \, dt \tag{3.6}$$

$$< \omega >= \int \frac{d\theta(t)}{dt} a(t)^2 dt \tag{3.7}$$

$$\omega = \frac{d\theta(t)}{dt} \tag{3.8}$$

Cohen suggests that the ω in the above expression be treated as instantaneous frequency. Instantaneous frequency should be treated as conditional average frequency. He also discussed a few paradoxes regarding instantaneous frequency. Some of these paradoxes are listed below:

- Instantaneous frequency may not be one of the frequencies in the spectrum!
- The spectrum of the analytic signal is zero for negative frequencies, the instantaneous frequency may be negative and hence loses its meaning.
- For a band-limited signal the instantaneous frequency may go outside the band.

Even after using the Hilbert Transform the definition of instantaneous frequency is controversial. The definition of ω as discussed in the previous equations is a mono-component function (single value function of time). At any given time, there exists one frequency value and it can represent only one component. However, this is not always true for non-stationary and non-linear signals that occur in nature.

Another more general definition for instantaneous frequency is given by Barnes [3] [8]:

$$\omega(t) = \frac{1}{2\Delta t} \arctan\left(\frac{x(t-\Delta t)y(t+\Delta t) - x(t+\Delta t)y(t-\Delta t)}{x(t-\Delta t)x(t+\Delta t) + y(t-\Delta t)y(t+\Delta t)}\right) \tag{3.9}$$

Where $y(t)$ is Hilbert Transform of $x(t)$ and Δt is the time between observations.

There are further restrictions on instantaneous frequency. Gabor suggests that for any function to have meaningful instantaneous frequency, the real part of its Fourier Transform has to have only positive frequency. Huang explains that the necessary conditions for us to define a meaningful instantaneous frequency are that the functions (IMFs) are symmetric with respect to the local zero mean, and have the same numbers of zero crossings and extrema. These are properties that Intrinsic Mode Functions (IMFs) satisfy.

3.2 Intrinsic Mode Functions

Huang has defined IMFs as signals satisfying the following conditions [13]:

- In the whole data set, the number of extrema and the number of zero crossings must either be equal or differ at most by one,
- At any point in the time series, the mean value of the envelope defined by local maxima and the envelope defined by the local minima is zero. In other words, the upper and lower envelope enclosing the signal should have zero mean.

An IMF represents a simple oscillatory mode as a counterpart to the simple harmonic function. IMFs retain the features of their parent data set and can uncover oscillatory trends that are not easily visible in the original. IMFs have well-behaved Hilbert Transform. Each IMF can be used to form analytic functions. This allows the IMFs themselves to be used for data analysis. Any time series can be reduced to IMF components from which an instantaneous frequency value can be assigned to each IMF component. The IMF in each cycle, defined by zero crossings, involves only one mode of oscillation. IMF is not restricted to a narrow band signal, and it can be both amplitude and frequency modulated. The second condition modifies the classical global requirement to a local one. [10]

3.3 Empirical Mode Decomposition

The basic concept of EMD is to identify proper time scales that reveal the physical characteristics of the signals, and then decompose the signal into IMFs (Intrinsic Mode Functions). The Empirical Mode Decomposition method in simplest terms is a filter that sifts through data and breaks it down into simpler components, the IMFs. EMD is an iterative process and the IMFs obtained from the sifting process are intrinsic to the signal, unlike the trigonometric basis in methods based on Fourier Spectral Analysis. So the basis of the decomposition is derived from the data. This breakdown is not based on random sinusoids and the original signal can be reconstructed as a sum of all the IMFs.

At any given time, the data may involve more than one oscillatory mode; that is why the simple Hilbert transform cannot provide the full description of the frequency content for the general data. So data needs to be decomposed into IMFs.

Assumptions for successful EMD [12]:

- The signal has at least two extrema—one maximum and one minimum;
- The characteristic time scale is defined by the time lapse between the extrema.
- If the data were totally devoid of extrema but contained only inflection points, then it can be differentiated once or more times to reveal the extrema. Final results can be obtained by integration(s) of the components

3.4 Working of EMD algorithm

EMD algorithm can be summarised in following steps [10] [12] :

1. The data $x(t)$ is examined for local maximum and minimum. Local maximas are joined by an upper envelope (cubic spline interpolation) and the same is done for local minima with a lower envelope. All the data points should be covered between these envelopes.

2. Mean of upper and lower envelope m_1 is calculated. Then, the difference between data $x(t)$ and the mean is calculated. This first difference h_1 is the first proto IMF component. This process of extracting IMFs is called the sifting process.

$$x(t) - m_1 = h_1 \tag{3.10}$$

3. This proto IMF h_1 is checked if it satisfies the conditions of IMFs stated earlier. If we have multiple extrema between successive zero crossings, then h_1 is not an IMF.

4. The sifting process needs to be repeated to eliminate anomalies such as multiple extremas between successive zero crossings. In the next iteration h_1 is treated as data and the sifting process is repeated.

$$h_1 - m_{11} = h_{11} \tag{3.11}$$

5. In subsequent iterations, the sifting process can be repeated k times until h_{1k} is an IMF component c_1. After k iterations, the first IMF component c_1 is obtained from the data. Provided the component satisfies the stoppage criteria.

$$h_{1(k-1)} - m_{1k} = h_{1k} \tag{3.12}$$
$$c_1 = h_{1k} \tag{3.13}$$

6. The Sifting process should be applied with care. Each iteration of the sifting process makes the mean approach zero. This also makes amplitude variations (intra-mode amplitude modulation) of the individual components constant. This results in components being the purely frequency-modulated signal. Then the resulting component would not retain any physically meaningful information.

7. The stoppage criteria determines the number of sifting steps required to produce an IMF. Huang et al. (1998) proposed the Standard Deviation SD from two consecutive sifting to be set between 0.2 and 0.3 [12]

$$SD = \sum_{t=0}^{T} \frac{|h_{1(k-1)}(t) - h_{1(k)}(t)|^2}{h^2_{1(k-1)}(t)} \tag{3.14}$$

8. The first stoppage criteria had a shortcoming that the value of SD can be dominated by local small values of h_{k-1}. Later Huang proposed an improved stopping criteria which he called the sum of the difference [10].

$$SD = \frac{\sum_{t=0}^{T} |h_{1(k-1)}(t) - h_{1(k)}(t)|^2}{\sum_{t=0}^{T} h^2_{1(k-1)}(t)} \tag{3.15}$$

9. Even with this new SD, the important criterion that the number of extrema has to equal the number of zero-crossings has not been checked. Huang et al. (2003) proposed an alternative stoppage criteria based on a number called S-number. S-number is defined as the number of consecutive siftings when the numbers of zero-crossings and extrema are equal or at most differing by one [14].

10. When the resulting component from the sifting process satisfies the stoppage criteria it is designated as the first IMF component c_1. Now first IMF component c_1, is separated from data $x(t)$. This results in a residue r_1.

$$x(t) - c_1 = r_1 \tag{3.16}$$

11. Residue r_1 still contains information about the longer period components. This residue is now treated as data and subjected to a sifting process. This process can be repeated on all subsequent residues r_js.

$$r_1 - c_2 = r_2 \tag{3.17}$$

$$r_{n-1} - c_n = r_n \tag{3.18}$$

12. The sifting process can be stopped if residue r_n becomes a monotonic function from which no more IMFs can be extracted or it is less than the predetermined value of the substantial consequence. Hence we achieved a decomposition of data $x(t)$ into n empirical modes (IMFs) and a residue r_n.

$$x(t) = \sum_{j=1}^{n} c_j + r_n \tag{3.19}$$

The first IMF component c_1 captures the highest frequency content. In the later IMF components, relevant frequency content decreases.

3.5 Hilbert Spectral Analysis

Hilbert transform was introduced by Mathematician David Hilbert for analytic functions. It is given by the following equation:

$$y(t) = \frac{P}{\pi} \int_{-\infty}^{\infty} \frac{x(\tau)}{x(t-\tau)} \, d\tau \tag{3.20}$$

$$z(t) = x(t) + iy(t) \tag{3.21}$$

where P is the Cauchy principal value, $y(t)$ is the imaginary part of analytic function $z(t)$ and $x(t)$ is the original input signal. The integration in Hilbert transform is not global but the convolution of $x(t)$ with $1/t$. This makes the result local. Hilbert transform phase shifts the actual data by 90-degree (multiplication by i). It enables the decomposition of the input signal $x(t)$ into its envelope and phase. Calculating envelope $a(t)$ and phase $\theta(t)$ is already discussed in the Instantaneous Frequency section.

Hilbert transform is a filtering operation that consists of two filters:

1. Hilbert Filter
2. Delay Filter

This transform is applied to the IMF components c_j's. This allows the computation of the instantaneous frequency and instantaneous energy in signal components (IMFs) and to determine the Hilbert spectrum. Signal $x(t)$ can be expressed in the following equation after applying the Hilbert transform on each IMF component:

$$x(t) = \sum_{j=1}^{n} a_j(t) e^{i \int \omega_j(t) \, dt} \tag{3.22}$$

This equation allows us to represent the amplitude $a_j(t)$ and instantaneous frequency $\omega_j(t)$ as functions of time. Notice that here both amplitude and instantaneous frequency are functions of time, unlike Fourier representation where both were constants. This joint time-frequency distribution is called Hilbert spectrum $H(t,\omega)$. IMF represents a generalized Fourier expansion where the basis is derived from the empirical decomposition of data $x(t)$ itself.

Some other useful definitions related to Hilbert spectral analysis are:

1. **Marginal spectrum**

$$h(\omega) = \int_0^T H(t, \omega)dt \tag{3.23}$$

   The marginal Spectrum represents the total amplitude contribution from each frequency value. The meaning of frequency in the marginal spectrum is different from frequency in Fourier-Spectral Analysis.

2. **Mean Marginal spectrum**

$$n(\omega) = \frac{1}{T}\int_0^T H(t, \omega)dt \tag{3.24}$$

3. **Instantaneous energy density**

$$IE(t) = \int_\omega H^2(t, \omega)d\omega \tag{3.25}$$

4. **Degree of stationarity**

$$DS(\omega) = \frac{1}{T}\int_0^T (1 - \frac{H(t, \omega)}{n(\omega)})^2 dt \tag{3.26}$$

   Higher the value of $DS(\omega)$, higher the process will be non-stationarity.

Example based on Hilbert Spectral Analysis

In this example, the Empirical Mode Decomposition (EMD) is applied to the audio signal from Sputnik shown in figure 2.7. Figure 3.1 shows the first 3 IMFs for that signal. Its marginal spectrum and Instantaneous Energy spectrum are also depicted in figure 3.2. Notice that the time-energy-frequency spectrum obtained from EMD and HSA is significantly better in time and frequency resolution as compared to the spectrogram.

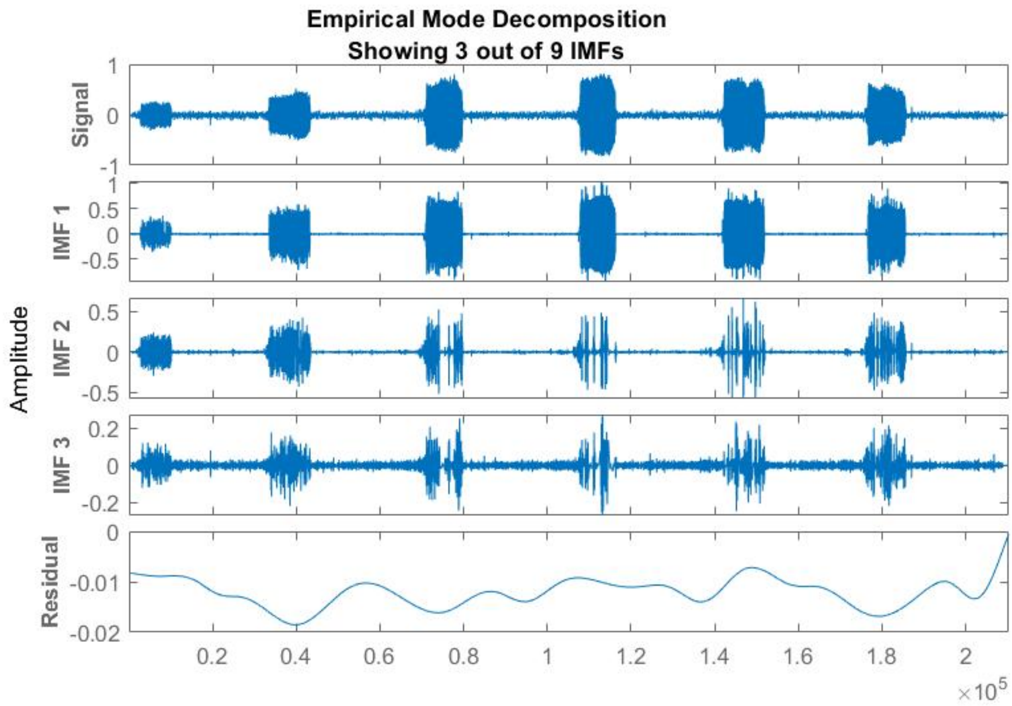

Figure 3.1: Empirical Mode Decomposition for audio of Sputnik 1

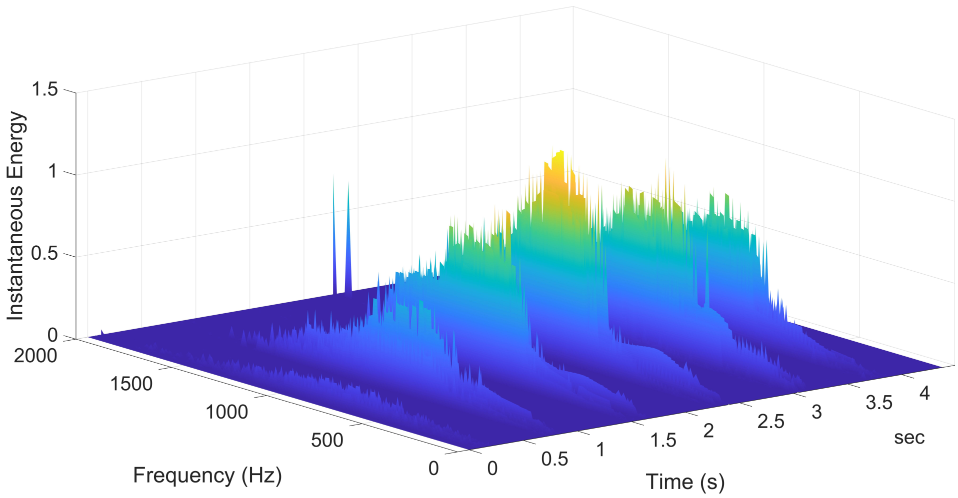

Figure 3.2: Hilbert Spectral Analysis for audio of Sputnik 1

CHAPTER 4

Application of Spectrogram and HHT to Synthetic Signals

4.1 Spectral analysis of signal displaying Beat Phenomenon

The beat phenomenon occurs when two signals with slightly different frequencies are superimposed. As a result, an oscillation with a slowly pulsating intensity is produced. Consider a signal composed of two sinusoids in equation 4.1 with frequency components of 30mHz and 33 mHz. This signal as shown in figure 4.1 exhibits the beat phenomenon when the two oscillatory modes are superimposed. Note that this is an example of additive inter-mode interaction.

$$x(t) = \sin\frac{2\pi}{30}t + 1.2\sin\frac{2\pi}{33}t \tag{4.1}$$

The signal shown in figure 4.1 was sampled at 125 mHz with 512 data points. In the Fourier spectrum of the signal shown in figure 4.2, the frequency components of 30mHz and 33 mHz can be identified (although with some leakage). EMD of signal as shown in figure 4.3 identifies the intrinsic time scales present in the signal but the IMFs c_1 and c_2 fails to give the exact frequency components and their magnitudes (30mHz and 33 mHz). This is a limitation of EMD in that it fails to decompose the signal when its frequency components are too close.

The spectrogram in figure 4.4 was produced using the Hanning window with 64 samples and 50 percent overlap. The minimum threshold was kept at -10 dB/Hz (for signal-to-noise ratio) for PSD to reject noise below this power level. No scaling factor for energy/amplitude is used since the absolute value of the amplitude is not the focus of the discussion.

On comparing the spectrogram in figure 4.4 and the Hilbert spectrum of the signal in figure 4.5, it is evident that the Hilbert spectrum gives a better resolution in time and frequency. Both the spectrogram and the EMD failed to resolve the frequency components of 30 and 33 mHz separately. This is due to the amplitude-modulated wave in the beat phenomenon. For superimposed signals with a given frequency and amplitude ratio, there exists a "confusion" frequency such that the two components cannot be separated. However, the frequency and temporal resolution in the Hilbert spectrum is still significantly better

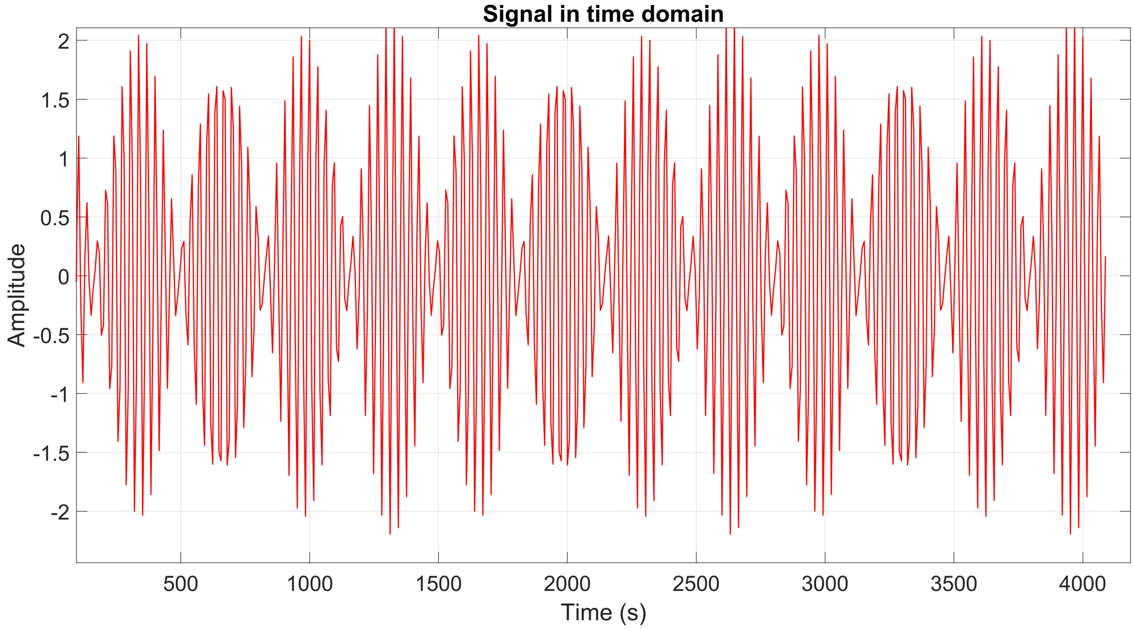

Figure 4.1: Signal displaying beat phenomenon

as compared to the spectrogram. This difficulty in tone separation is discussed by Patrick Flandrin, for more details see [17].

Huang's explanation for this behavior is the severe contamination of IMFs by spline fitting in the sifting process. It is not possible to improve the frequency resolution (getting the distinct waves/frequency components) by increasing the number of data points in the analysis. Huang recommends the use of higher-order splines in order to get better results. For a known stationary time series Fourier analysis seems a better option!

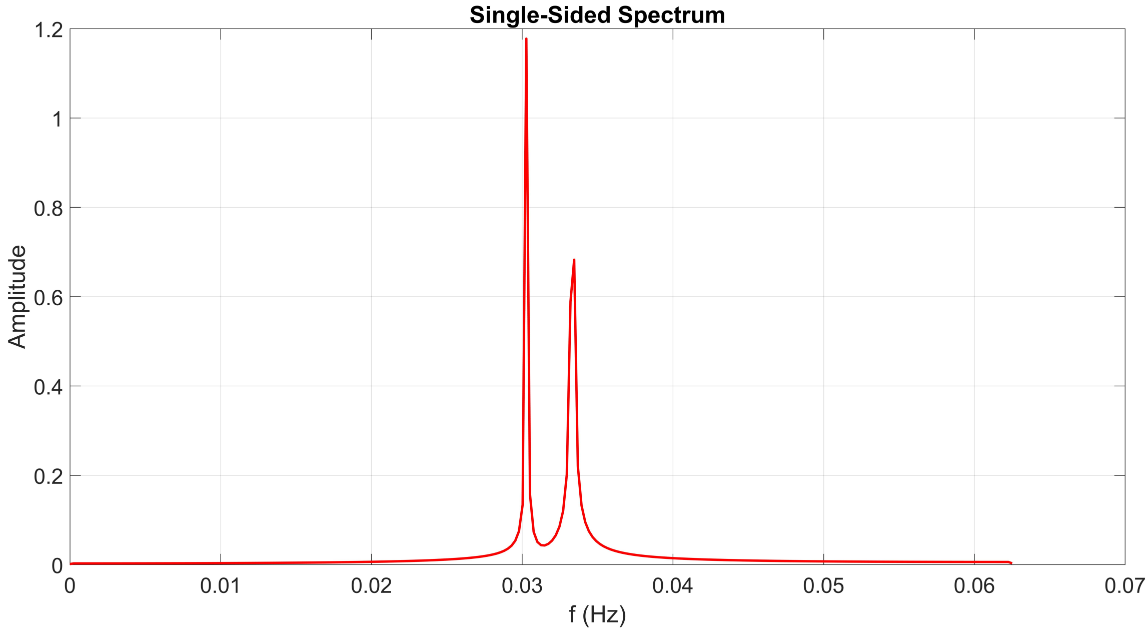

Figure 4.2: Fourier Spectrum of the signal displaying beat phenomenon

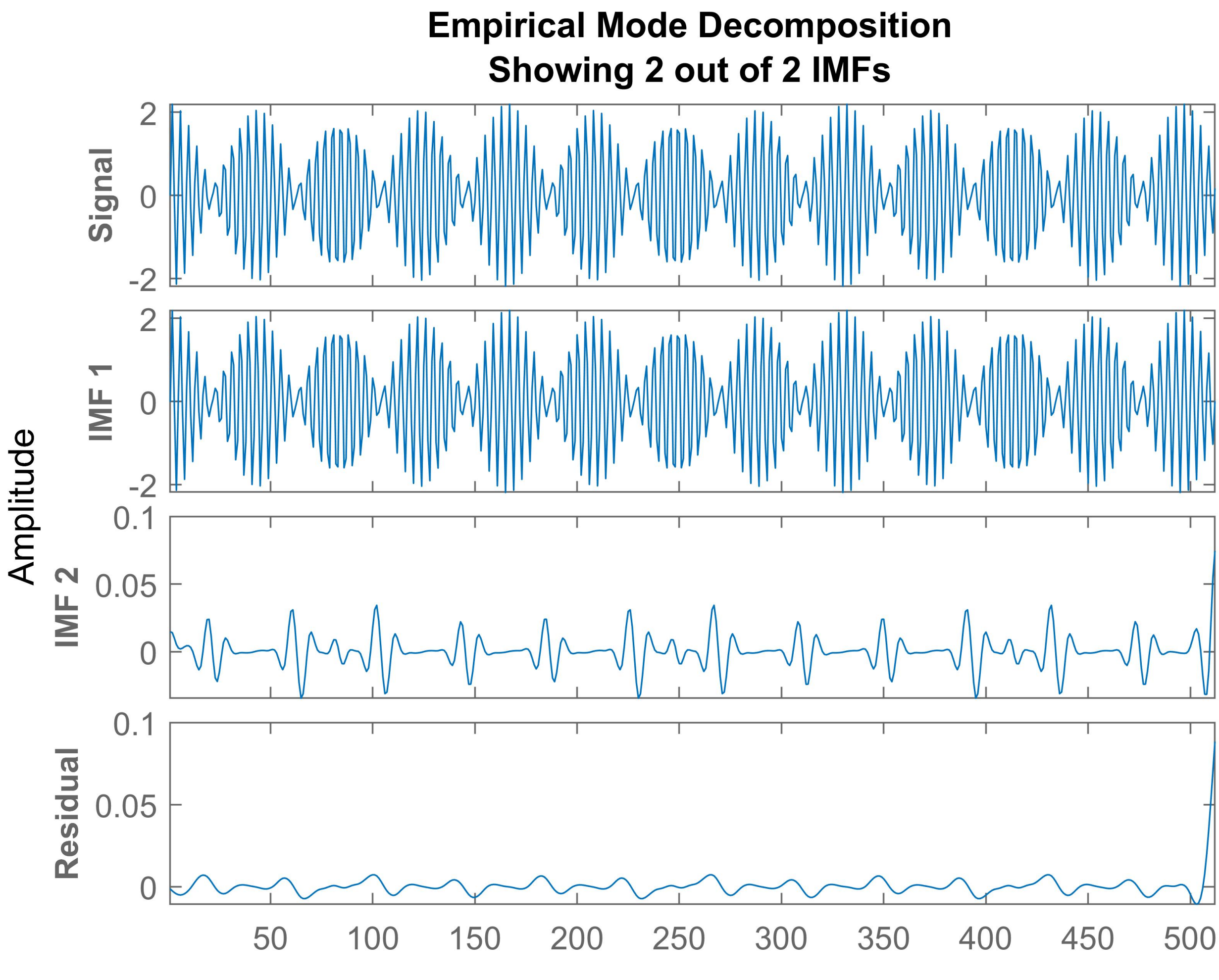

Figure 4.3: Empirical Mode Decomposition of the signal displaying beat phenomenon

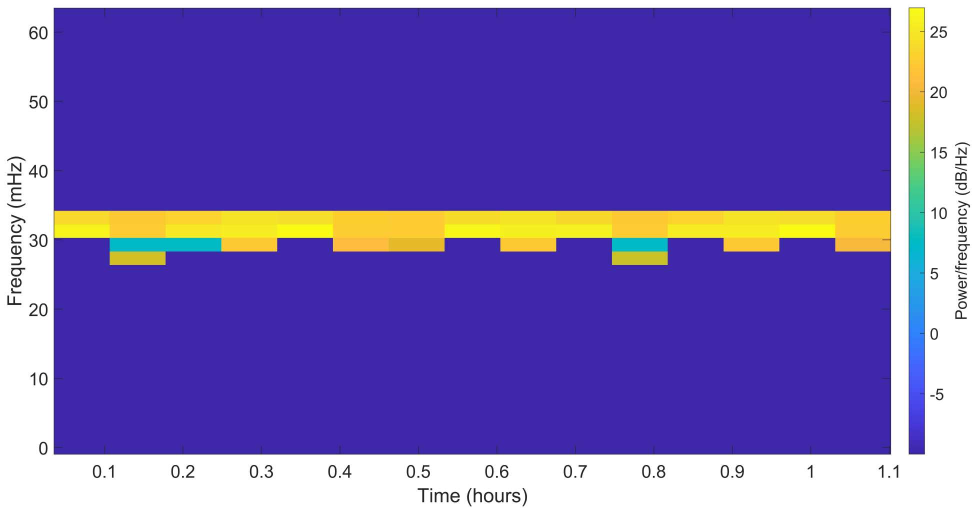

Figure 4.4: Spectrogram of signal displaying beat phenomenon

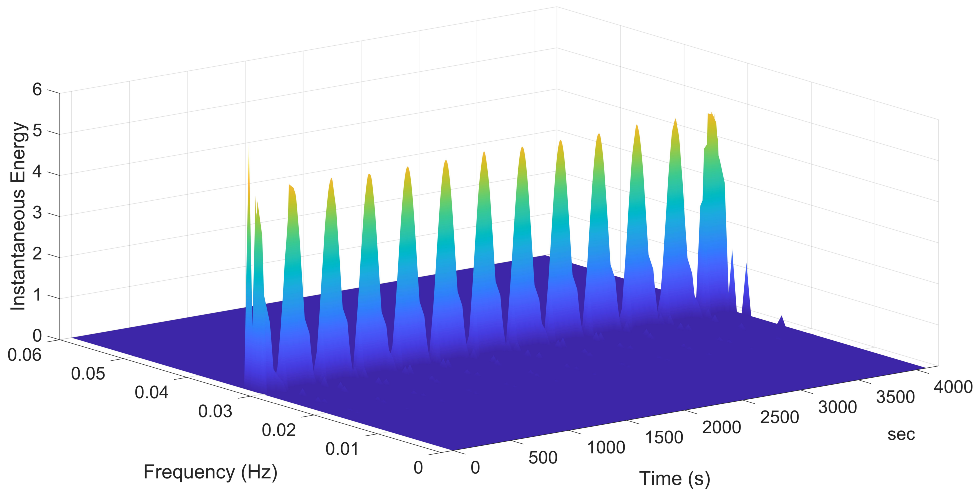

Figure 4.5: Instantaneous energy and Hilbert spectrum of signal displaying beat phenomenon

4.2 Spectral analysis of non-stationary non-linear signals

Consider the signal described by the equation 4.2. It is composed of two sinusoids with frequencies 30 mHz and 40mHz and an exponential decay. This signal as shown in figure 4.6 is obtained by multiplicative inter-mode interaction between signal components and an exponential decay. It exhibits non-linearity by multiplicative interaction of modes and non-stationarity by exponential decay, hence it is a non-stationary non-linear signal (NSNL).

$$x(t) = e^{-0.001t} \sin \frac{2\pi}{33} t \times \sin \frac{2\pi}{25} t + Noise \tag{4.2}$$

The Fourier spectrum of the signal is obtained by using 2048 samples sampled at 0.5 Hz. For the spectrogram of this signal, the Hanning window is used with 64 samples and fifty percent overlap. In the Fourier spectrum of this signal as shown in figure 4.7 and the spectrogram as shown in figure 4.8, it can be noticed that the dominant frequencies are 10 mHz and 70 mHz not the expected 30 mHz and 40 mHz! This can be explained by the use of trigonometric identities, it is known that:

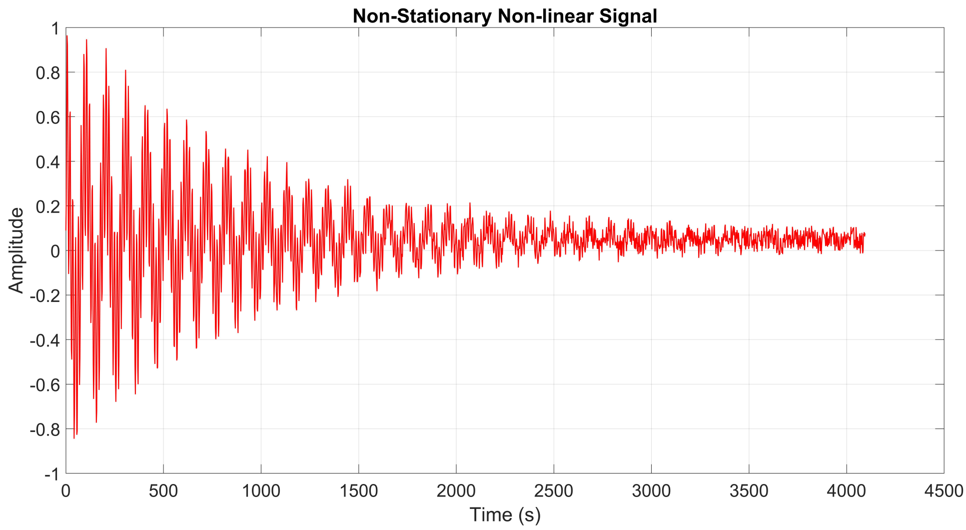

Figure 4.6: Non-stationary Non-linear signal

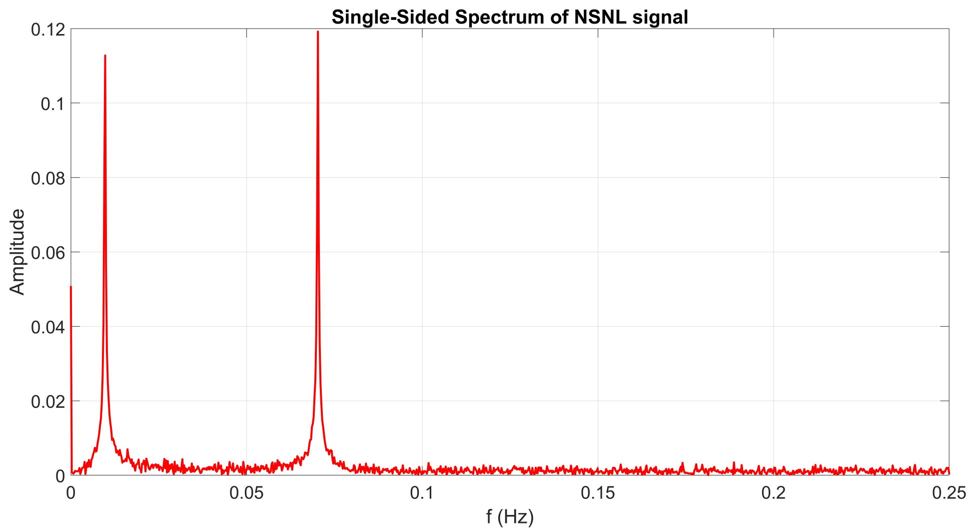

Figure 4.7: Fourier spectra of the Non-stationary Non-linear signal

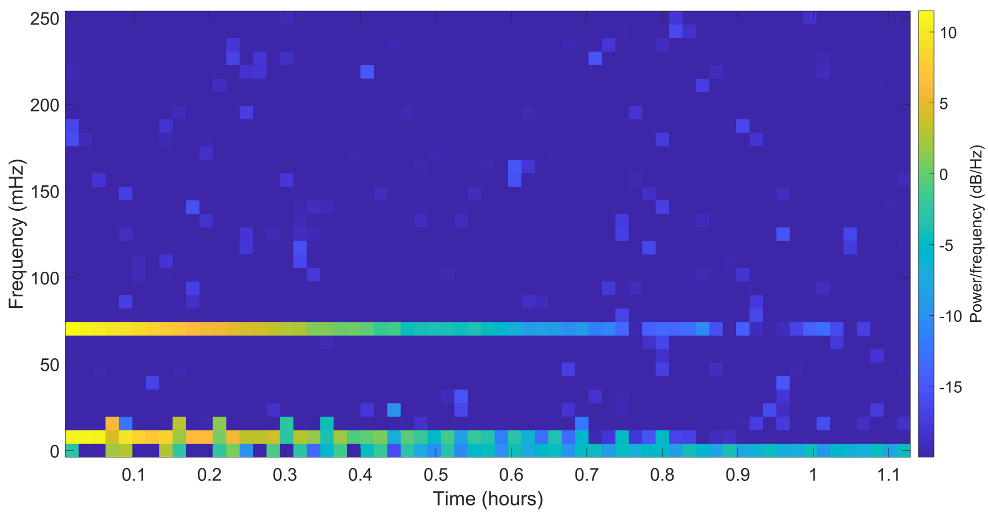

Figure 4.8: Spectrogram of the Non-stationary Non-linear signal

$$\sin a \sin b = \frac{1}{2}[\cos{(a-b)} - \cos{(a+b)}] \tag{4.3}$$

Substituting a = 40 mHz and b = 30 mHz, we get the mathematical explanation of why the frequencies 10 mHz (40-30) and 70 mHz (30+40) appear in the spectrum instead of the expected 30 mHz and 40mHz. Mathematically it makes perfect sense but physically it is meaningless since 10 mHz and 70 mHz do not exist in the signal and the spectrum obtained is misleading!

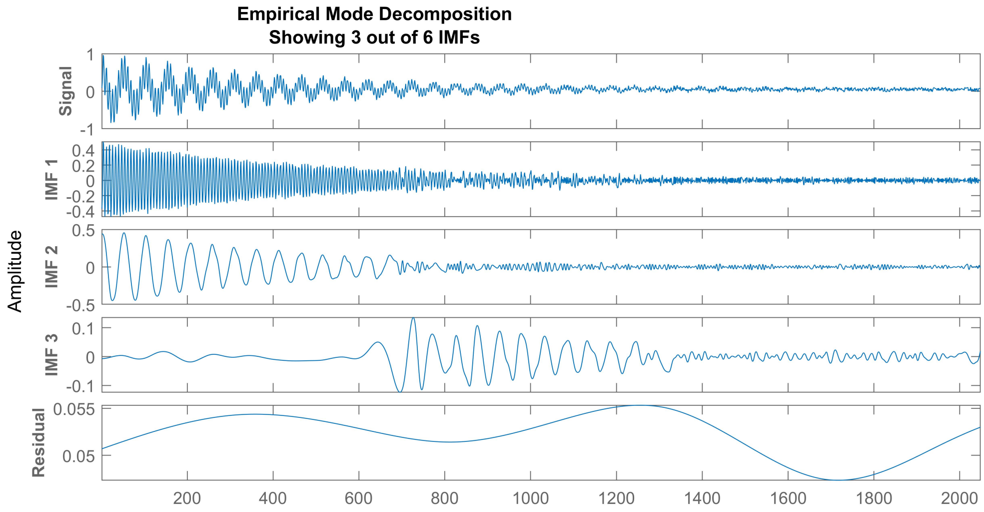

Figure 4.9: Empirical Mode Decomposition of the Non-stationary Non-linear signal

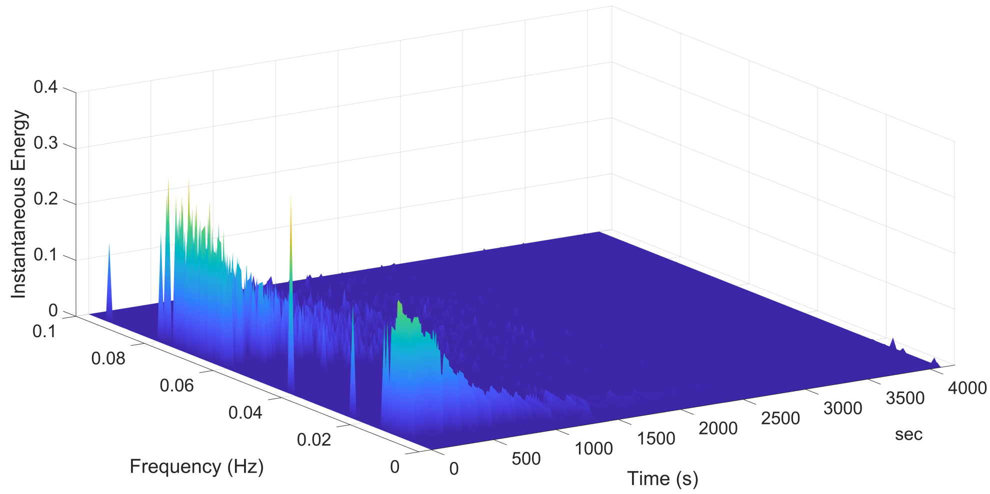

Figure 4.10: Hilbert spectra of the Non-stationary Non-linear signal

Even the EMD fails to resolve this issue of misleading frequencies as shown in figure 4.9 and figure 4.10 showing Hilbert spectral analysis of the signal. Fourier spectral analysis is perfectly capable of extracting the modes when there is additive interaction between signal components. But when it comes to multiplicative interaction between modes, both spectrogram and Hilbert Spectral Analysis (HSA) fail! HHT is capable of dealing with intra-mode interactions but not inter-mode interactions. This problem of inter-mode non-linear interactions is further aggravated when the number of multiplicative interactions is increased in the signal. This critical deficiency of additive decomposition methods is discussed in detail by Huang et al. using Holo-Hilbert spectral analysis [11].

CHAPTER 5

Application of Spectrogram and HHT to Wind Turbine Data

5.1 Introduction

The dataset used for analysis in this chapter was obtained from the sensors on the offshore wind turbines. This dataset is part of a research project "In-Situ-Wind" at the Chair of Mechanics, University of Siegen. More information about the project can be found here: In-Situ-Wind.

5.2 Methodology

5.2.1 Data Structure and Preliminary Analysis

The dataset contains sensor data from sensors like accelerometers, strain gauges, temperature, pressure, and wind speed sensors. There are two distinct datasets named D1 and D2 obtained on different dates. Both these datasets contain data from 3 sensor groups - comp1, comp2, and comp4. comp1 refers to the controller of the sensors in the grout area of the wind turbine, comp2 refers to the controller in the tower area and comp4 contains SCADA data of the Wind turbine like wind speed, rotation and, Environmental Operational Conditions (EOC). The data structure with detailed information about measuring units, sampling frequency, and sensor description is shown in the figure 5.1.

The sensor data was extracted from MATLAB data structure into small individual CSV data files for doing analysis independent of the software suite/packages. These CSV files were labeled according to the naming scheme and variable names. Figure 5.2 shows this with an example of the EOC dataset. For example, a CSV file named **D2C4SG1** refers to dataset 2, controller 4 (SCADA data), and the sensor group 1. For acceleration datasets obtained from the accelerometers, the following naming scheme was used for naming variables. Variables $Acc1_x, Acc1_y, Acc1_z$ means acceleration data from accelerometer sensor 1 for the x,y, and z axis.

The analysis was mainly done on the acceleration datasets from the sensors in the grout

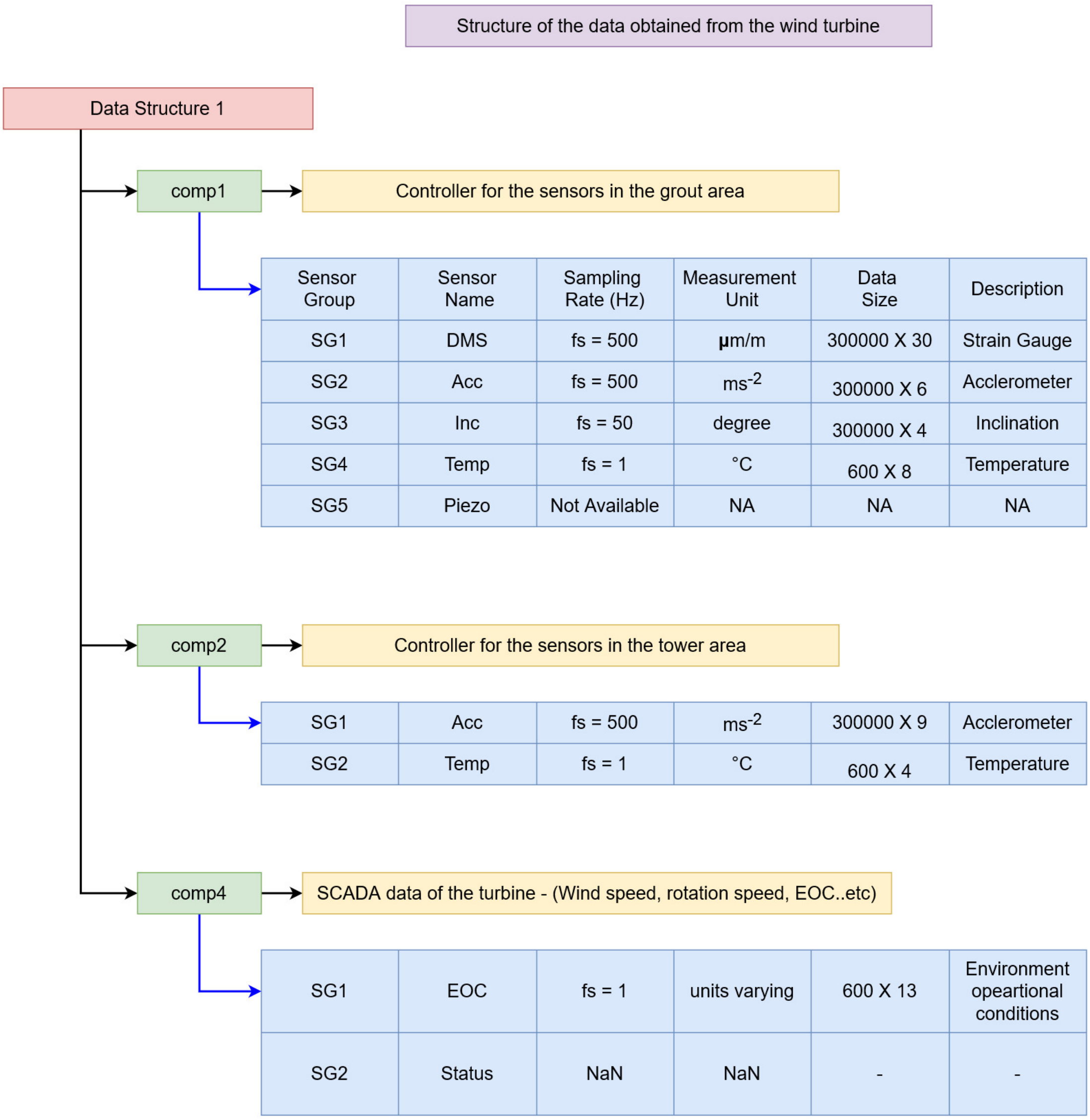

Sensor Group	Sensor Name	Sampling Rate (Hz)	Measurement Unit	Data Size	Description
SG1	DMS	fs = 500	μm/m	300000 X 30	Strain Gauge
SG2	Acc	fs = 500	ms^{-2}	300000 X 6	Acclerometer
SG3	Inc	fs = 50	degree	300000 X 4	Inclination
SG4	Temp	fs = 1	°C	600 X 8	Temperature
SG5	Piezo	Not Available	NA	NA	NA

SG1	Acc	fs = 500	ms^{-2}	300000 X 9	Acclerometer
SG2	Temp	fs = 1	°C	600 X 4	Temperature

SG1	EOC	fs = 1	units varying	600 X 13	Environment opeartional conditions
SG2	Status	NaN	NaN	-	-

Figure 5.1: Structure of sensor data obtained from offshore Wind Turbine

Environmental Operational Conditions Dataset (SCADA Data)		
Symbol/Variable	**Description**	**Units**
Amb_temp	Ambient temperature	°C
Wind_speed	Wind speed	rpm
Yaw_direction	Yaw direction	degrees
Rotor_rpm	Rotor speed	rpm
Generator_rpm	Generator speed	rpm
Blade_angle_ref	Blade angle reference	degree
Blade_angle_a	Blade angles	degree
Blade_angle_b	Blade angles	degree
Blade_angle_c	Blade angles	degree
Blade_pres	Blade pressure	bar
Active_power	Active power	kW
Reactive_power	Reactive power	kVAr
Available_power	Available power	kW

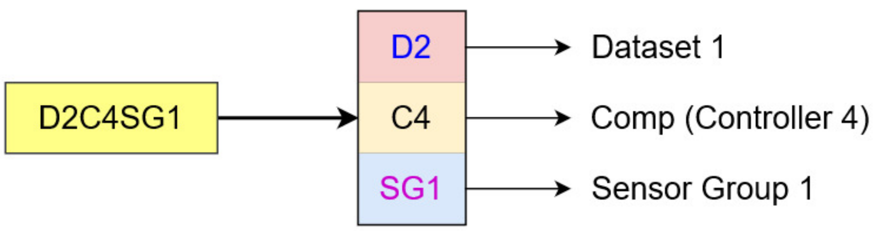

Figure 5.2: Environment Operational Conditions Dataset

area as well as the tower area. EOC data like temperature, wind speed, and blade rotation speed collected by the SCADA system were found not suitable for this application after doing the preliminary analysis. Acceleration data is primarily obtained from accelerometer sensors in the grout area [data size = (300000 X 6) | no. of sensors = 2] and the tower area [data size = (300000 X 9) | no. of sensors = 3]. The sampling frequency for all the accelerometers was 500 Hz for a total period of 600 seconds in both datasets D1 and D2. For consistency in benchmarking the performance of the spectrogram with Hilbert Spectral Analysis(HSA), the following design parameters were established after a few trials and errors: Spectrogram - [window size = 128, overlap = 50 percent, window type = Hanning], EMD and HSA [No. of IMFs = 6 to 9, and frequency limits = 0-250 Hz]. Acceleration data was made zero mean by subtracting the mean value of acceleration from all the data vectors. This step was necessary because HHT needs zero mean data to work efficiently. For Fourier analysis, this is equivalent to removing the DC component.

The Matlab codes perform the following tasks for the acceleration datasets:

- Imports the CSV file and assigns the column vectors variable names according to the naming scheme.
- Create plots of acceleration data as time series for the x,y, and z axes.
- Calculate the mean value of acceleration datasets and subtract this mean from the entire vectors to make it zero mean.
- Performs the FFT for x,y, and z data vectors and plots the frequency spectrum.
- Create the spectrograms with pre-decided parameters.
- Performs EMD on the input vectors, applies Hilbert spectral analysis on the resulting IMFs, and then creates a 3-D Hilbert Spectrum of time-frequency-instantaneous energy.
- Repeats the entire process for all the acceleration sensors 1,2, 3 ... and so on.

5.3 Data Analysis Results

The figures 5.3, 5.4, 5.5 5.6, 5.7, and 5.8 shows the acceleration data in the time domain and the frequency domain for the z,y, and the x-axis respectively. For this sensor, it is evident that the dominating frequency components are around 20 Hz and 161 Hz.

Comparing the spectrograms in the figure 5.9, 5.10, and 5.11 with the respective results of EMD and subsequent Hilbert spectral analysis in the figures 5.12, 5.13, and 5.14 it can be seen that EMD and HSA offer better time-frequency resolution. However, it was noticed that EMD and HSA required more computational resources in terms of calculation time and memory compared to the Spectrograms. For more detailed explanations of the computational complexity of the empirical mode decomposition algorithm see [21]

The same methodology was applied to all other acceleration datasets and a similar conclusion was reached based on comparative data analysis results. That a combination of EMD and HSA provides better time-frequency resolution at the cost of computing resources. Since the datasets and the number of images produced are too large, not all the results are shown in this report. The detailed results with the codes and high-resolution images can be found here in the repository: HHT- Spectrogram In-Situ-Wind.

Analysis of Dataset: D1C1SG2 - Acceleration sensor 1 in the grout area

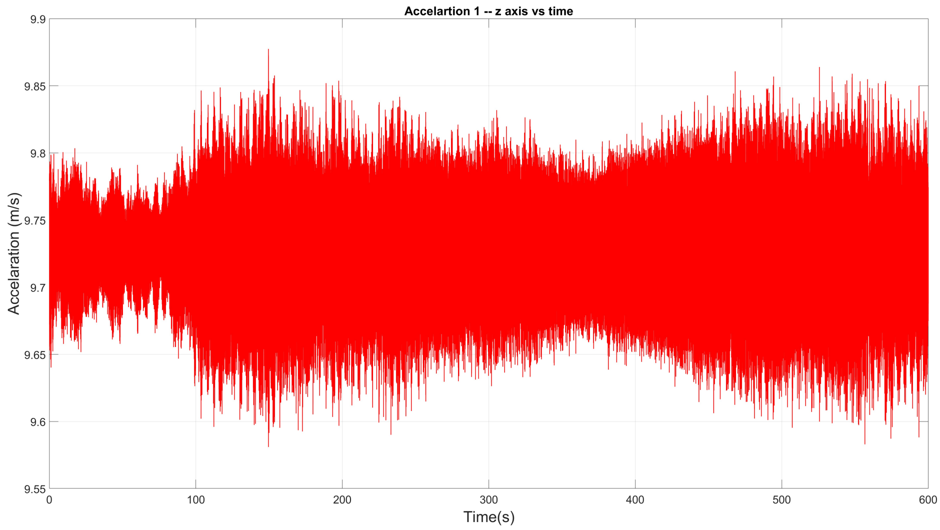

Figure 5.3: Sensor 1 acceleration signal – z axis in time domain

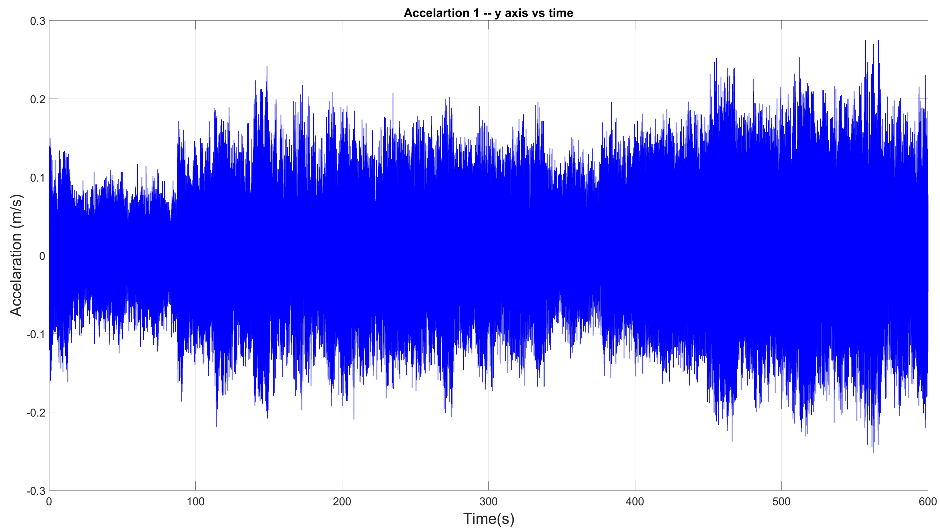

Figure 5.4: Sensor 1 acceleration signal – y axis in time domain

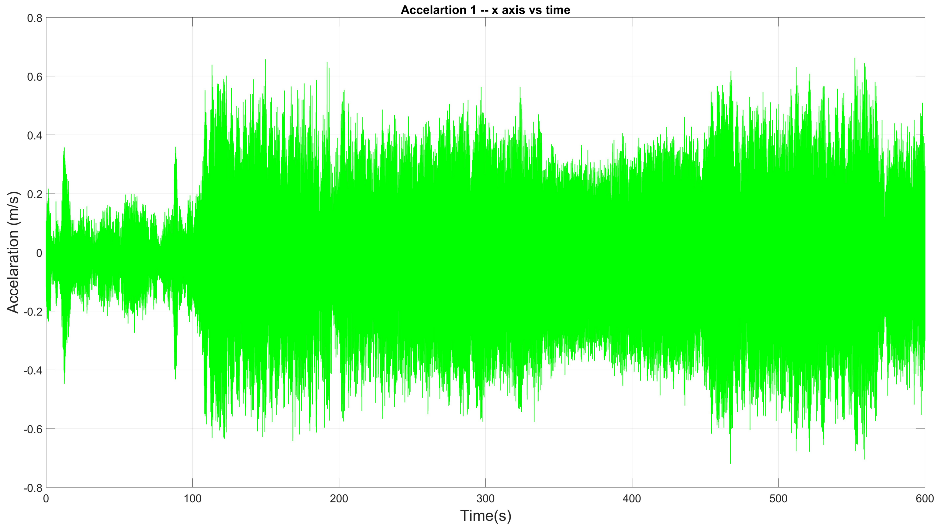

Figure 5.5: Sensor 1 acceleration signal – x axis in time domain

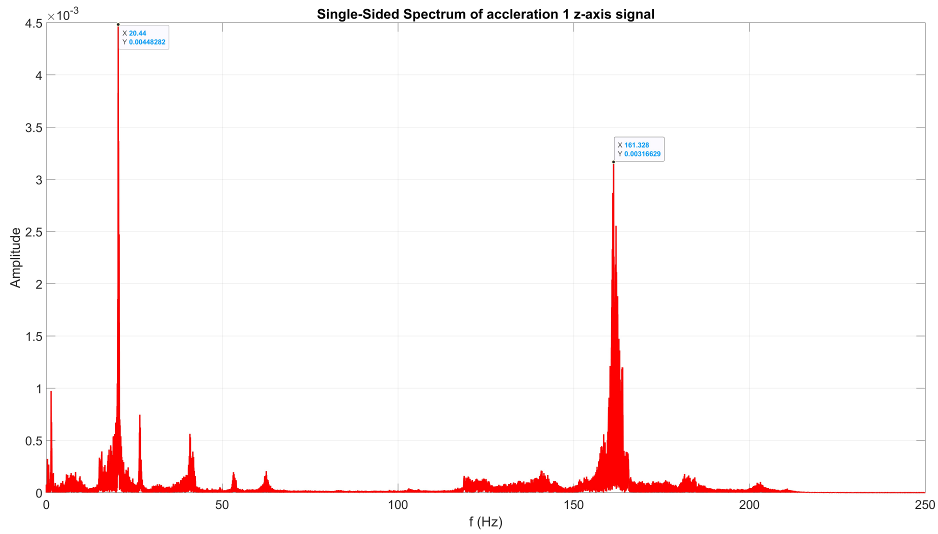

Figure 5.6: Sensor 1 acceleration signal – z axis Frequency Spectrum

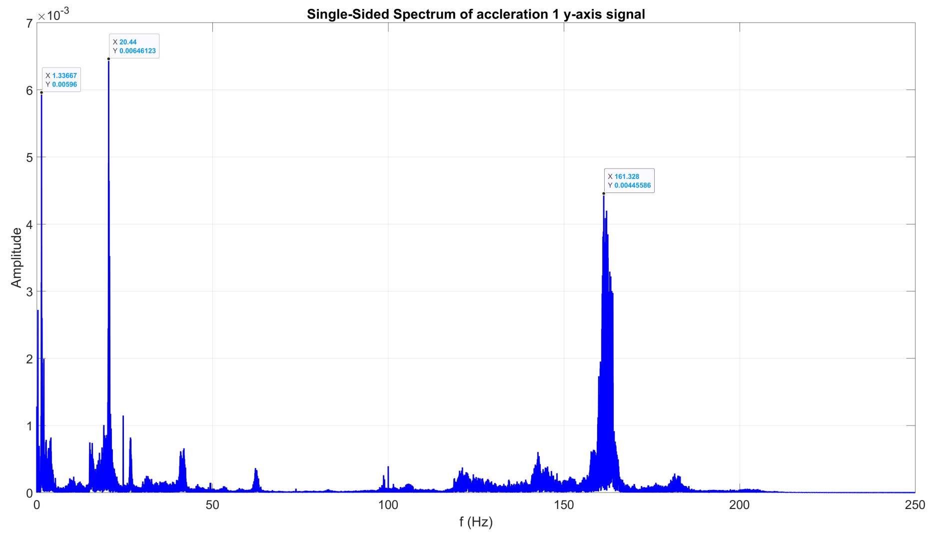

Figure 5.7: Sensor 1 acceleration signal – y axis Frequency Spectrum

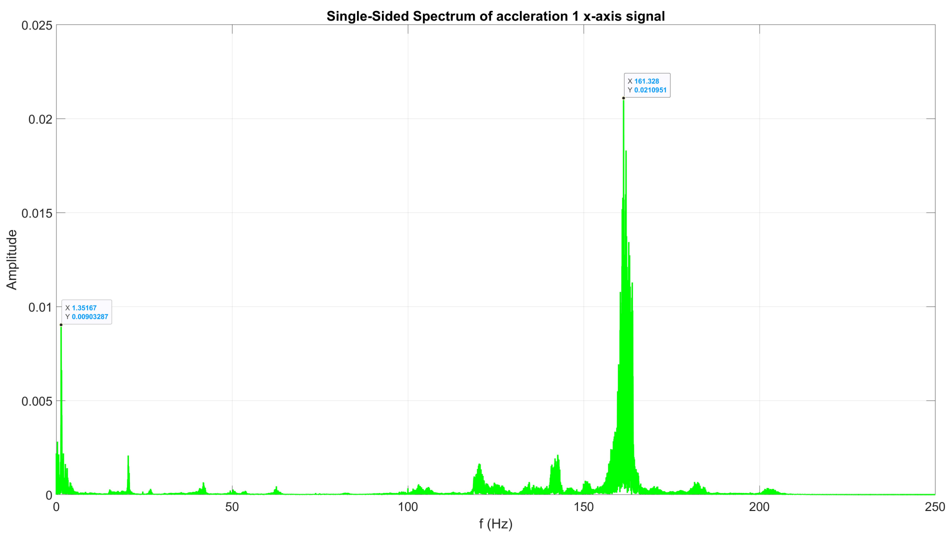

Figure 5.8: Sensor 1 acceleration signal – x axis Frequency Spectrum

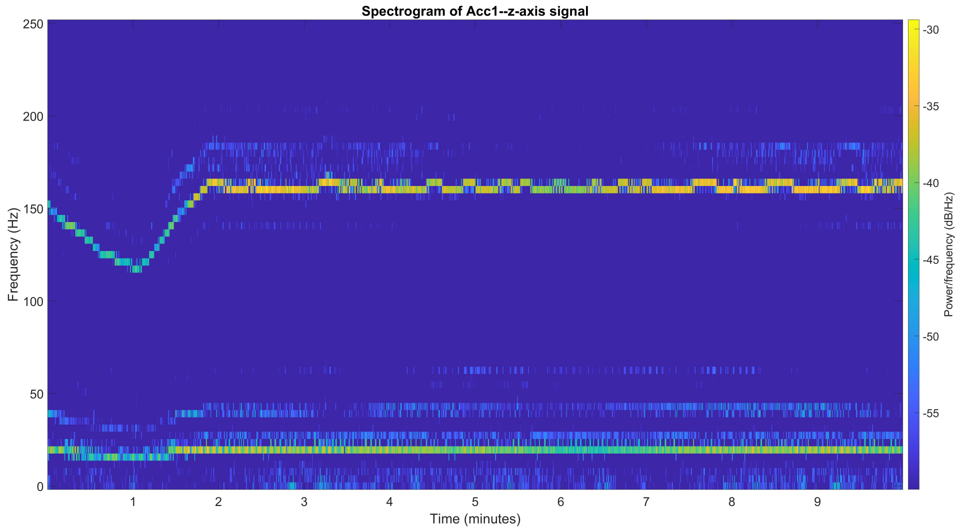

Figure 5.9: Sensor 1 acceleration signal – z axis Spectrogram

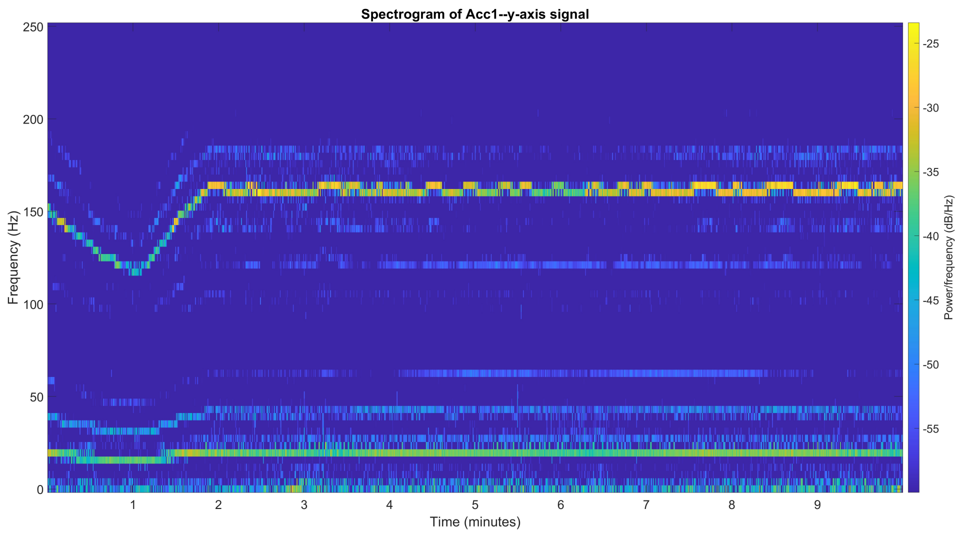

Figure 5.10: Sensor 1 acceleration signal – y axis Spectrogram

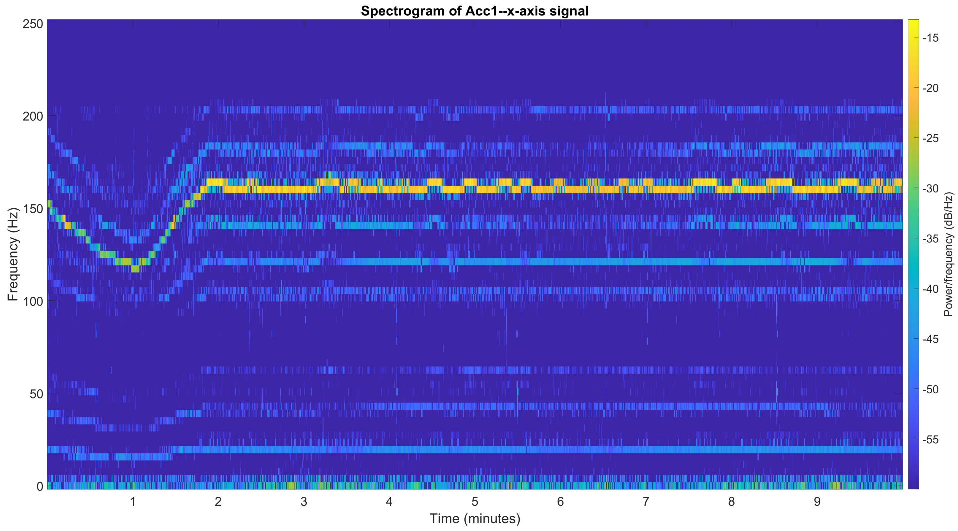

Figure 5.11: Sensor 1 acceleration signal – x axis Spectrogram

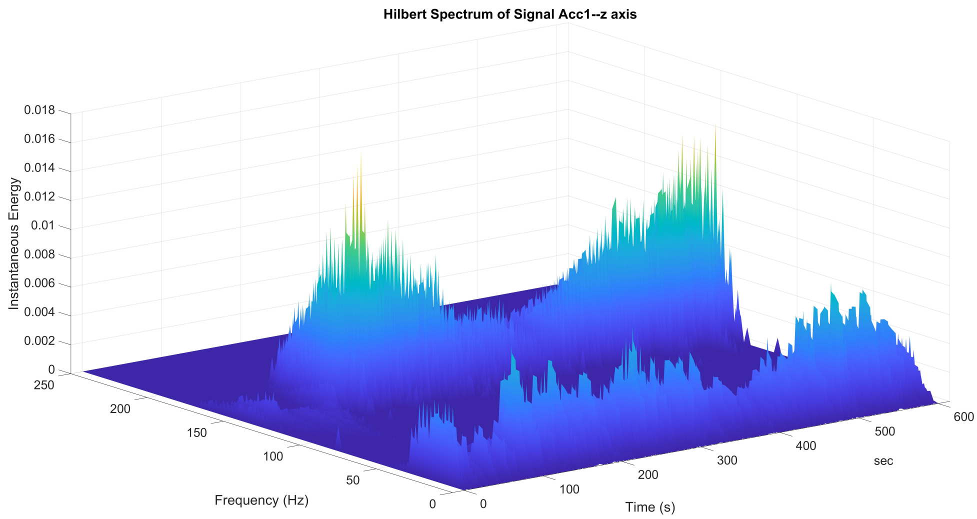

Figure 5.12: Sensor 1 acceleration signal – z axis Hilbert Spectrum

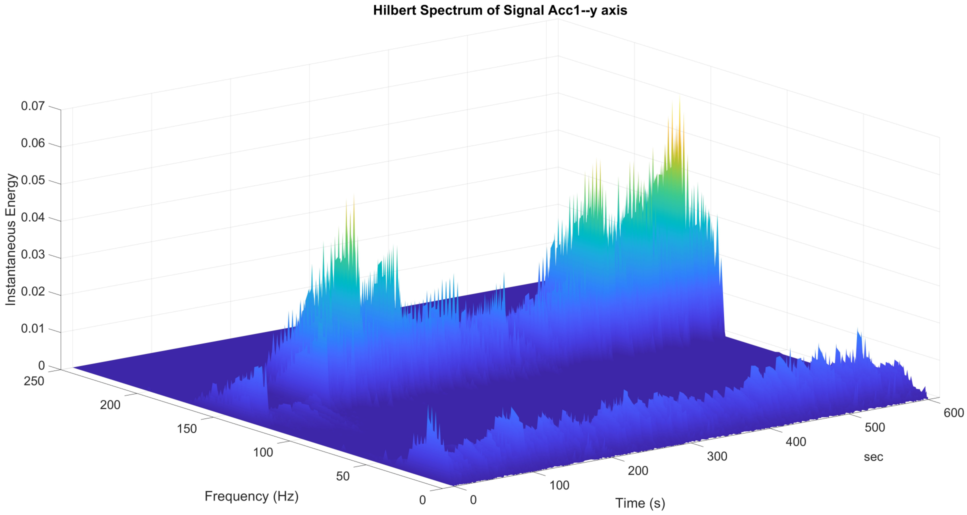

Figure 5.13: Sensor 1 acceleration signal – y axis Hilbert Spectrum

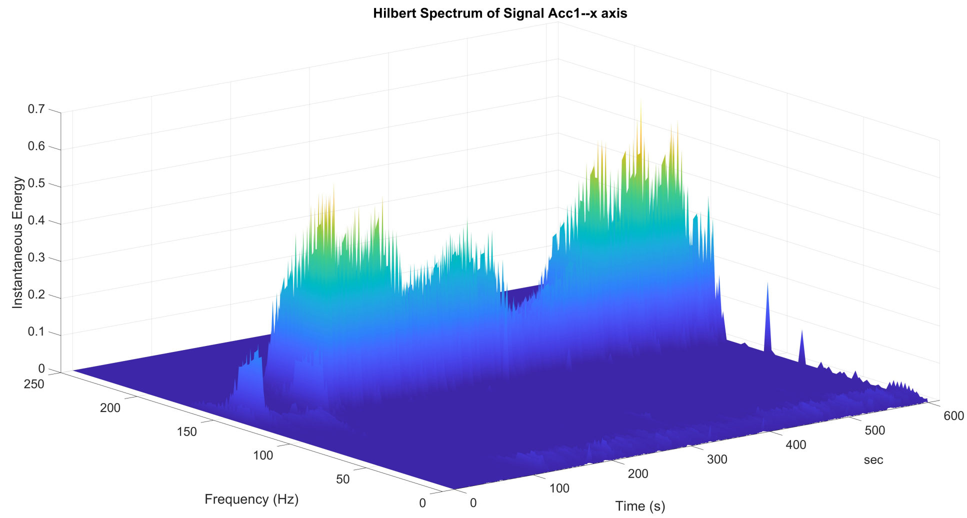

Figure 5.14: Sensor 1 acceleration signal – x axis Hilbert Spectrum

CHAPTER 6

Conclusion

The combination of Empirical Mode Decomposition and Hilbert Spectral Analysis in HHT has shown great promise in extracting the modes from non-stationary and non-linear signals. However there are some limitations associated with EMD. These limitations are listed below :

6.1 Limitations of signal processing based on Hilbert Huang Transform

1. For strictly linear and stationary data, Fourier spectral analysis produce better results. EMD cannot separate signals when their frequencies are too close. This is shown in the example of signal displaying beat phenomenon.
2. For many signals EMD does not converge down to a set of finite IMFs.
3. EMD algorithm involves cubic spline fitting to capture extremas. This spline fitting has both overshoot and undershoot problems and needs improvements. Higher order spline fitting have been used by Huang and others but it leads to only marginal improvements with increased computational costs.
4. The end effects both in spline fitting and Hilbert transform need improvements.
5. EMD is an algorithm, all inferences drawn from it are empirical. Individual IMF components obtained from EMD does not guarantee a well defined physical meaning but it provides a very realistic insight into data.
6. The key idea behind the EMD is to identify the inherent time scales in data. Unlike Fourier analysis, the basis derived from the data (IMFs) in EMD are not always orthogonal. Although in most cases these derived basis from EMD (IMFs) are practically orthogonal.
7. In Fourier analysis, Nyquist frequency required at-least 2 data points per wave. However Hilbert transform needs over-sampled data to define instantaneous frequency

precisely. For HHT Huang recommends 4-5 data points to define the frequency more accurately.

8. HHT can deal with intra-mode interactions but fails with inter-mode multiplicative interactions. This difficulty is addressed by advancements like Holo-Hilbert spectral analysis.

For a more detailed review of limitations associated with EMD and HHT see [2] [16].

6.2 Recent advances in HHT and EMD

This section enumerates some key areas where recent advancements in HHT have taken place. Traditional EMD suffers from problems like mode mixing, analysis of signals with closely spaced frequency components, sensitivity to noise/artifacts, and analysis of signals with multi channel measurement. To deal with these problems some variants of EMD like Ensemble EMD (EEMD), Multivariate EMD (MEMD), Normalized Hilbert Transform (NHT), and Holo-Hilbert Spectral Analysis were developed. These methods and developments are listed briefly.

Normalized Hilbert Transform (NHT):

Normalized Hilbert Transform is a variant of standard HHT that uses a normalization factor in computing the instantaneous frequency. It improves on the limitations of singularity and normalization of HT. For more details on NHT see [9].

Multivariate EMD (MEMD):

MEMD is an extension of EMD that uses projections in multiple directions on unit hyperspheres (n-spheres) for the analysis of multi-channel data. This method addresses the challenge of computing the local mean in multivariate signals in the standard EMD algorithm. For generating these direction vectors, MEMD uses uniform angular sampling and quasi-Monte Carlo methods. For in-depth understanding of MEMD see [18] [19] [20].

Ensemble EMD (EEMD):

Ensemble EMD was introduced to overcome the limitations of standard EMD algorithm in analysis of noisy data. EEMD consists of sifting an ensemble of white noise-added signal (data) and treats the mean as the final true result. It offers several advantages over standard EMD algorithm such as:

- Reduction of Mode Mixing: By introducing randomness through the addition of white noise, EEMD helps to mitigate mode mixing and other artifacts that may arise in the decomposition process.
- Enhanced Robustness: Ensemble averaging improves the robustness of the decomposition method to noise and other sources of variability in the data.
- Denoising: Ensemble averaging effectively reduces the noise level in the resulting decomposition, leading to better signal-to-noise ratio in the extracted IMFs.

For more details on EEMD and EEMD based methods see [22] [15].

Holo-Hilbert Spectral Analysis (HHSA):

The HHSA was introduced to overcome the limitations of HHT like inter-mode amplitude and frequency modulations. It uses a nested EMD and HHT approach to identify intrinsic amplitude and frequency modulations in nonlinear systems. It provides a multidimensional representation of data, capturing both additive and multiplicative, intra-mode and inter-mode interactions. It distinguishes between linear additive and nonlinear multiplicative processes, addressing the inability of existing methods to represent multiplicative interactions. For more details see [11].

Bibliography

[1] François Auger, Patrick Flandrin, Paulo Gonçalvès, and Olivier Lemoine. Time-frequency toolbox. *CNRS France-Rice University*, 46, 1996.

[2] Mohamed Barbosh, Premjeet Singh, and Ayan Sadhu. Empirical mode decomposition and its variants: A review with applications in structural health monitoring. *Smart Materials and Structures*, 29(9):093001, 2020.

[3] Arthur E Barnes. The calculation of instantaneous frequency and instantaneous bandwidth. *Geophysics*, 57(11):1520–1524, 1992.

[4] AJAA Bekele. Cooley-tukey fft algorithms. *Advanced algorithms*, 2016.

[5] Steven L Brunton and J Nathan Kutz. *Data-driven science and engineering: Machine learning, dynamical systems, and control.* Cambridge University Press, 2022.

[6] Leon Cohen. *Time-frequency analysis*, volume 778. Prentice hall New Jersey, 1995.

[7] James W Cooley and John W Tukey. An algorithm for the machine calculation of complex fourier series. *Mathematics of computation*, 19(90):297–301, 1965.

[8] Dean G Duffy. The application of hilbert–huang transforms to meteorological datasets. *Journal of Atmospheric and Oceanic Technology*, 21(4):599–611, 2004.

[9] Norden E Huang. Computing instantaneous frequency by normalizing hilbert transform. *United States Patent, US 6,901,353 B1*, 2005.

[10] Norden E Huang and Nii O Attoh-Okine. *The Hilbert-Huang transform in engineering.* CRC Press, 2005.

[11] Norden E Huang, Kun Hu, Albert CC Yang, Hsing-Chih Chang, Deng Jia, Wei-Kuang Liang, Jia Rong Yeh, Chu-Lan Kao, Chi-Hung Juan, Chung Kang Peng, et al. On holo-hilbert spectral analysis: a full informational spectral representation for nonlinear and non-stationary data. *Philosophical Transactions of the Royal Society A: Mathematical, Physical and Engineering Sciences*, 374(2065):20150206, 2016.

[12] Norden E Huang, Zheng Shen, Steven R Long, Manli C Wu, Hsing H Shih, Quanan Zheng, Nai-Chyuan Yen, Chi Chao Tung, and Henry H Liu. The empirical mode decomposition and the hilbert spectrum for nonlinear and non-stationary time series analysis. *Proceedings of the Royal Society of London. Series A: mathematical, physical and engineering sciences*, 454(1971):903–995, 1998.

[13] Norden E Huang, Man-Li Wu, Wendong Qu, Steven R Long, and Samuel SP Shen. Applications of hilbert–huang transform to non-stationary financial time series analysis. *Applied stochastic models in business and industry*, 19(3):245–268, 2003.

[14] Norden E Huang, Man-Li C Wu, Steven R Long, Samuel SP Shen, Wendong Qu, Per Gloersen, and Kuang L Fan. A confidence limit for the empirical mode decomposition and hilbert spectral analysis. *Proceedings of the Royal Society of London. Series A: Mathematical, Physical and Engineering Sciences*, 459(2037):2317–2345, 2003.

[15] Xun Lang, Naveed ur Rehman, Yufeng Zhang, Lei Xie, and Hongye Su. Median ensemble empirical mode decomposition. *Signal Processing*, 176:107686, 2020.

[16] RT Rato, Manuel Duarte Ortigueira, and AG Batista. On the hht, its problems, and some solutions. *Mechanical systems and signal processing*, 22(6):1374–1394, 2008.

[17] Gabriel Rilling, Patrick Flandrin, Paulo Goncalves, et al. On empirical mode decomposition and its algorithms. In *IEEE-EURASIP workshop on nonlinear signal and image processing*, volume 3, pages 8–11. Citeseer, 2003.

[18] Gabriel Rilling, Patrick Flandrin, Paulo Gonçalves, and Jonathan M Lilly. Bivariate empirical mode decomposition. *IEEE signal processing letters*, 14(12):936–939, 2007.

[19] Naveed ur Rehman and Danilo P Mandic. Empirical mode decomposition for trivariate signals. *IEEE Transactions on signal processing*, 58(3):1059–1068, 2009.

[20] Naveed ur Rehman, Cheolsoo Park, Norden E Huang, and Danilo P Mandic. Emd via memd: multivariate noise-aided computation of standard emd. *Advances in adaptive data analysis*, 5(02):1350007, 2013.

[21] Yung-Hung Wang, Chien-Hung Yeh, Hsu-Wen Vincent Young, Kun Hu, and Men-Tzung Lo. On the computational complexity of the empirical mode decomposition algorithm. *Physica A: Statistical Mechanics and its Applications*, 400:159–167, 2014.

[22] Zhaohua Wu and Norden E Huang. Ensemble empirical mode decomposition: a noise-assisted data analysis method. *Advances in adaptive data analysis*, 1(01):1–41, 2009.

[23] Gengsheng Lawrence Zeng and Megan Zeng. Fourier series. In *Electric Circuits*, pages 157–170. Springer, 2021.